PRECEDING PAGE BLANK NOT FILMED.

FINAL REPORT

DESIGN AND DEVELOP A HIGH DENSITY MEMORY SYSTEM

for

National Aeronautics and Space Administration
George C. Marshall Space Flight Center
Huntsville, Alabama 35812

Contract No. NAS8-20755
(DCN 1-7-40-7962)

SUBMITTED BY: Heinz Lienhard
Heinz Lienhard,
Project Engineer

APPROVED BY: Irving Wolf
Irving W. Wolf, Manager
Materials and Devices
Research Department

Ampex Corporation
401 Broadway
Redwood City, California 94063

PRECEDING PAGE BLANK NOT FILMED.

SUMMARY

It was the scope of the present work to prove the feasibility of producing high density memory planes based on a closed flux structure developed by Ampex.

Since the digit line density is only fabrication-limited, it was important to show that very fine memory lines can be produced. Digit lines of .5 mil and .25 mil width have been successfully etched; a memory line density of 1000 lines per inch or even more will, therefore, be feasible.

The word line density is limited by demagnetization and creep effects. It has been demonstrated that the following bit densities are possible:

1000Å film: 166,000 bits/inch^2

500Å film: 250,000 bits/inch^2

In a two-spots-per-bit configuration these density figures have to be divided by two.

Electronic test results were obtained by working with wider digit lines. The memory arrays for electronic evaluation were scaled in a way to give conclusive results for the high density planes.

PRECEDING PAGE BLANK NOT FILMED.

CONTENTS

CONTENTS (Cont)

1.0 INTRODUCTION

Matrices of thin magnetic films are well-known for high speed storage purposes. There are two basic types of film memories now being explored: those using planar films for storage, and those using cylindrical films.

1.1 Planar Films

Planar magnetic films of high quality can be made relatively thin (e.g., 100Å) whereby self-demagnetization effects are reduced. Any magnetic domain in a planar film is, by its nature, an open flux configuration. Therefore, demagnetization effects near the edges of a planar domain prove to be a threat to the stability of a memory cell. This situation can be somewhat improved by juxtaposing two cells which are magnetized anti-parallel (sandwich).

1.2 Cylindrical Film

Where a magnetic film is deposited onto a wire with its easy axis along the circumference, there is no problem of flux closure. The surface roughness of wires and rods leads to a comparatively high anisotropy dispersion (i.e., poor film quality). In addition, the surface quality of state-of-the-art substrates has limited the deposition of magnetic films to thicknesses higher than 5000Å.

Although such a thickness yields a larger sense signal, severe demagnetization and creep problems result which impair the stability of stored information and allow but very low packaging densities. Furthermore, cylindrical films present a severe handling problem because their substrate - a relatively thin wire - is much less rigid than the substrates used for planar films.

1.3 New Closed Flux Structure

A new thin film structure has been developed which combines the advantages of a planar film with those of the cylindrical film but does not suffer from the severe drawbacks of the two approaches. The new structure allows high switching speeds and lends itself for a higher density memory.

2. 0 DESCRIPTION OF THE DEVICE

2. 1 Closed Flux Memory Lines

Figure 1 shows the cross section of such a structure. Notice the two permalloy layers NiFe #1 and NiFe #2, both of which can be fabricated with a very high surface quality typical of good planar magnetic films. Sandwiched between the permalloy is a copper conductor which will serve as a combined bit-sense line.

A last permalloy layer NiFe #3 closes the flux. Such a structure may be called a "plated wire analog."

Adjacent lines do not interact even if they are spaced very closely. The flux closure, on one hand, prevents static field interference between memory cells. The field produced by the central copper conductor, on the other hand, is shown in Fig. 2. Note that the field acting on the adjacent magnetic line has hardly any horizontal component and thus is insignificant. Therefore, the packing density of these magnetic lines will be limited by the present fabrication technology; and it is not as is the case for both conventional planar and cylindrical film memories limited by interaction problems.

2. 2 Memory Array

The "plated wire analog" described has a continuous coating of magnetic material. In order to subdivide the storage medium along one line, a set strip line conductor can be placed orthogonally to the magnetic lines as shown in Fig. 4. These lines may be fabricated in a batch process

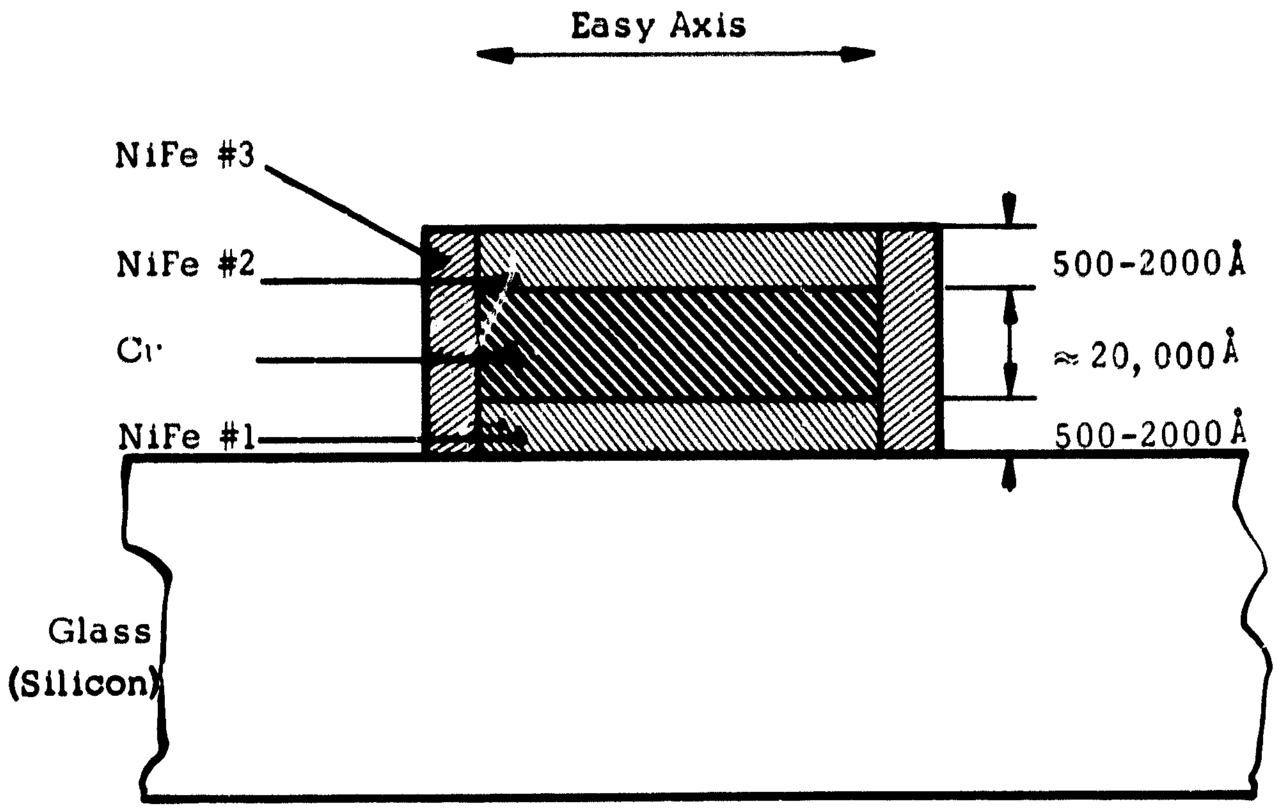

Fig. 1 Geometry of Closed Flux Storage Cell

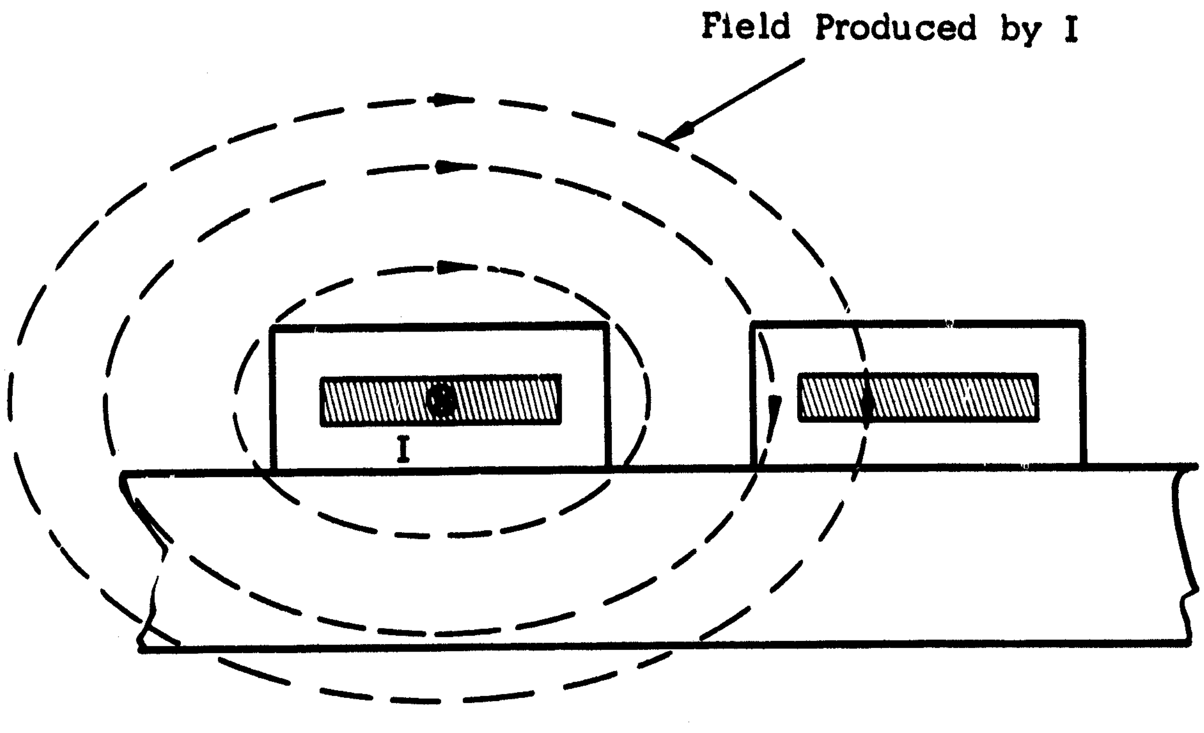

Fig. 2 Interaction Between Adjacent Cells

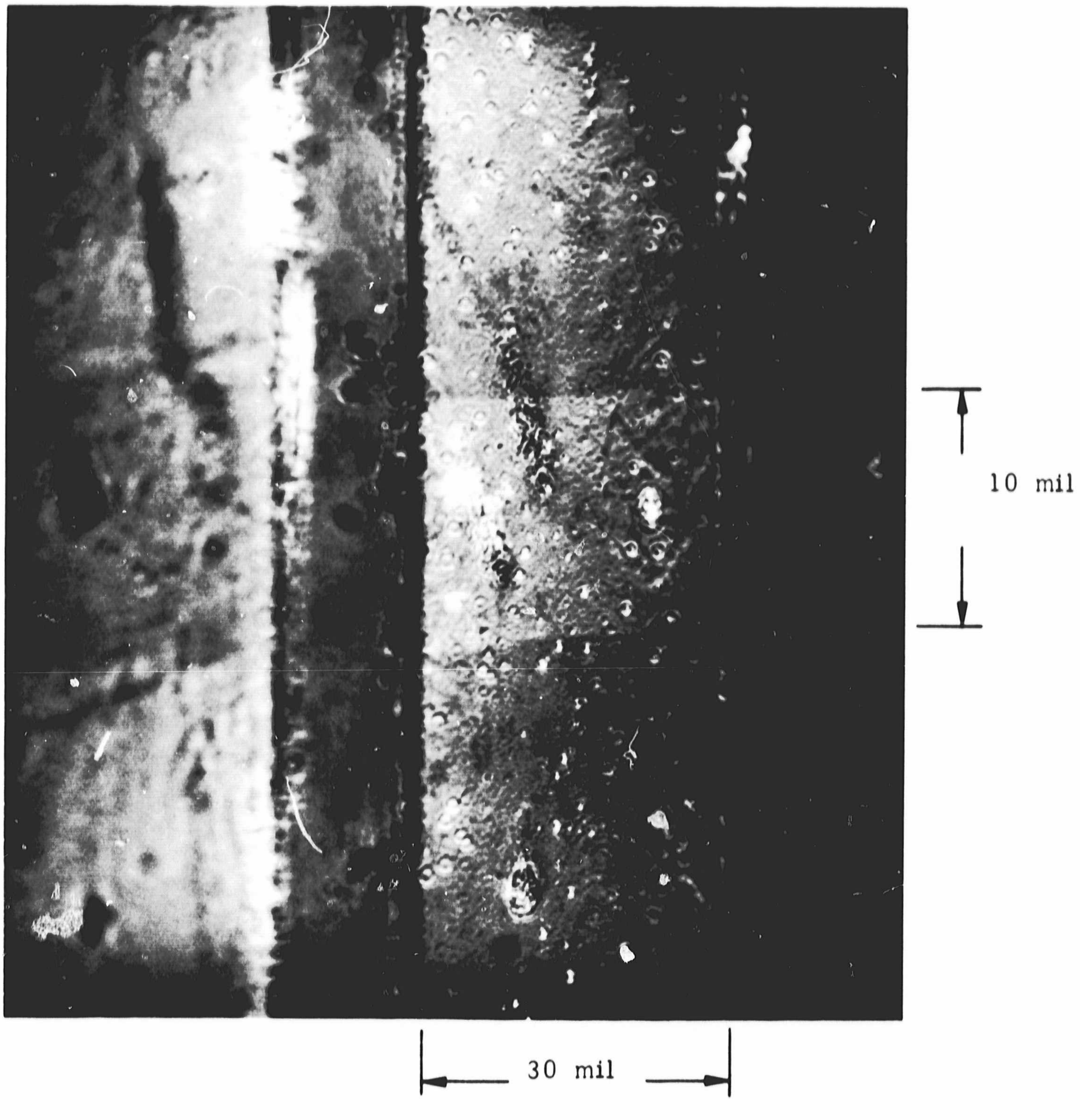

Fig. 3 Kerr-Magneto-Optic Observation of Domain with Closed Flux

similar to the first set. In the scheme proposed, they will be deposited onto a separate substrate, preferably flexible tape. As registration of the two substrates is uncritical, the two substrates may simply be brought in close proximity. The magnetic domain carrying 1 bit of information in Fig. 3 has been written in this way.

In the arrangement of Fig. 4, the strip conductor inside the closed flux structure will be operated as a combined bit-sense line. The orthogonal strip lines in turn will be operated as word lines.

The size and spacing of the word lines are limited by creep and demagnetization phenomena in the magnetic medium. The word lines must therefore be larger than the bit lines.

The properties of this type of magnetic film device lend themselves best to a word-organized memory matrix. Because all lines are very narrow

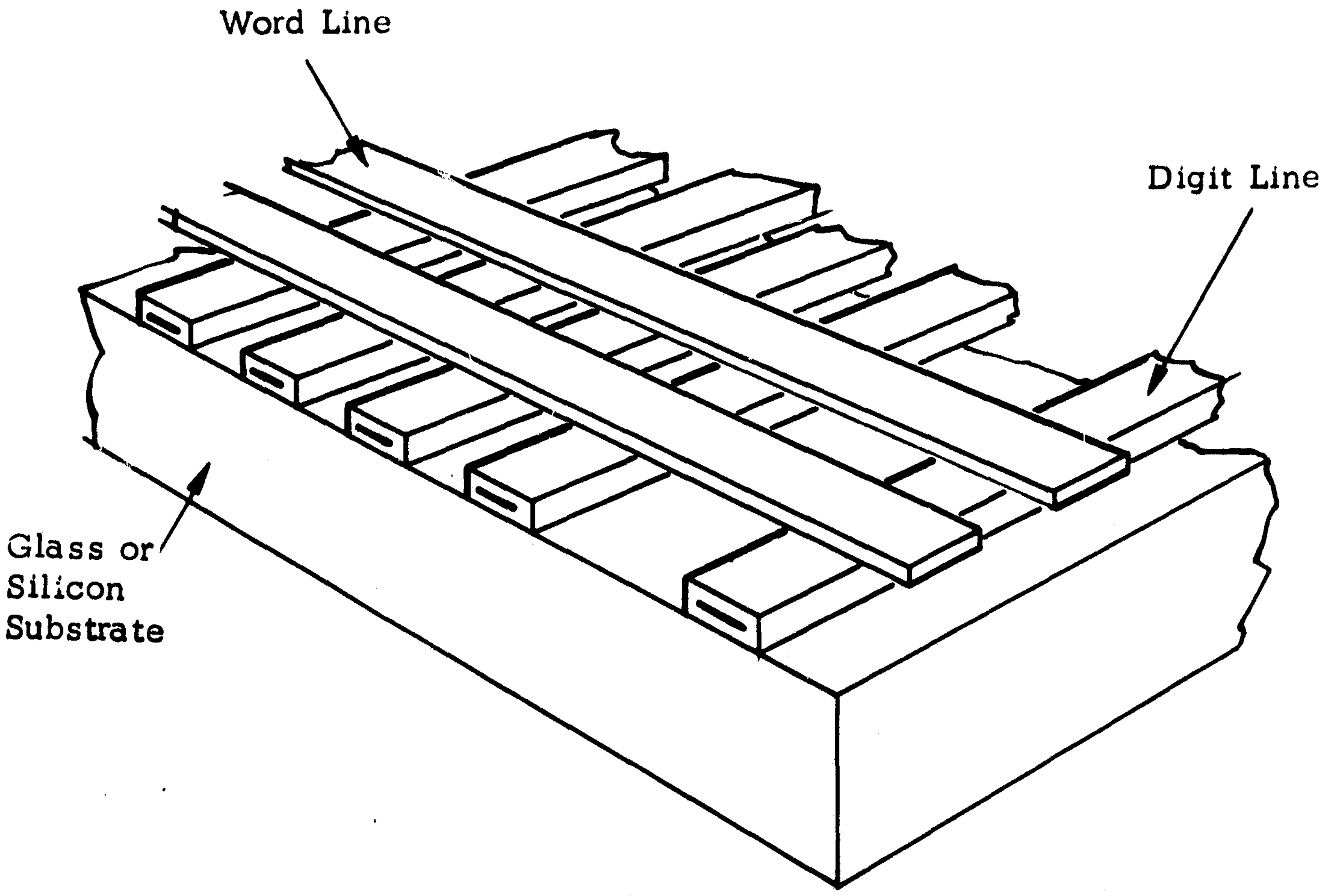

Fig. 4 Array of Closed Flux Storage Cells

and the coupling of the field they produce to the magnetic film is very tight, the current pulses needed are small.

2.3 High Density Memory Plane

Digit line density is essentially fabrication-limited. It has been proved during the course of this work that etching of 0.5 to 0.25 mil wide memory lines is possible. Thus a line density of 1000 lines per inch is made feasible.

Word line density is limited by demagnetization and creep effects. It has been found (see Chapter 4) that 3 mil wide word drive lines 3 mils apart are feasible to drive 1000Å thick films yielding a word line density of approximately 170 lines per inch. If thinner films and consequently lower signals can be tolerated, then the word line density can be increased accordingly. Figure 5 shows the high density memory structure based on a 1000Å permalloy film.

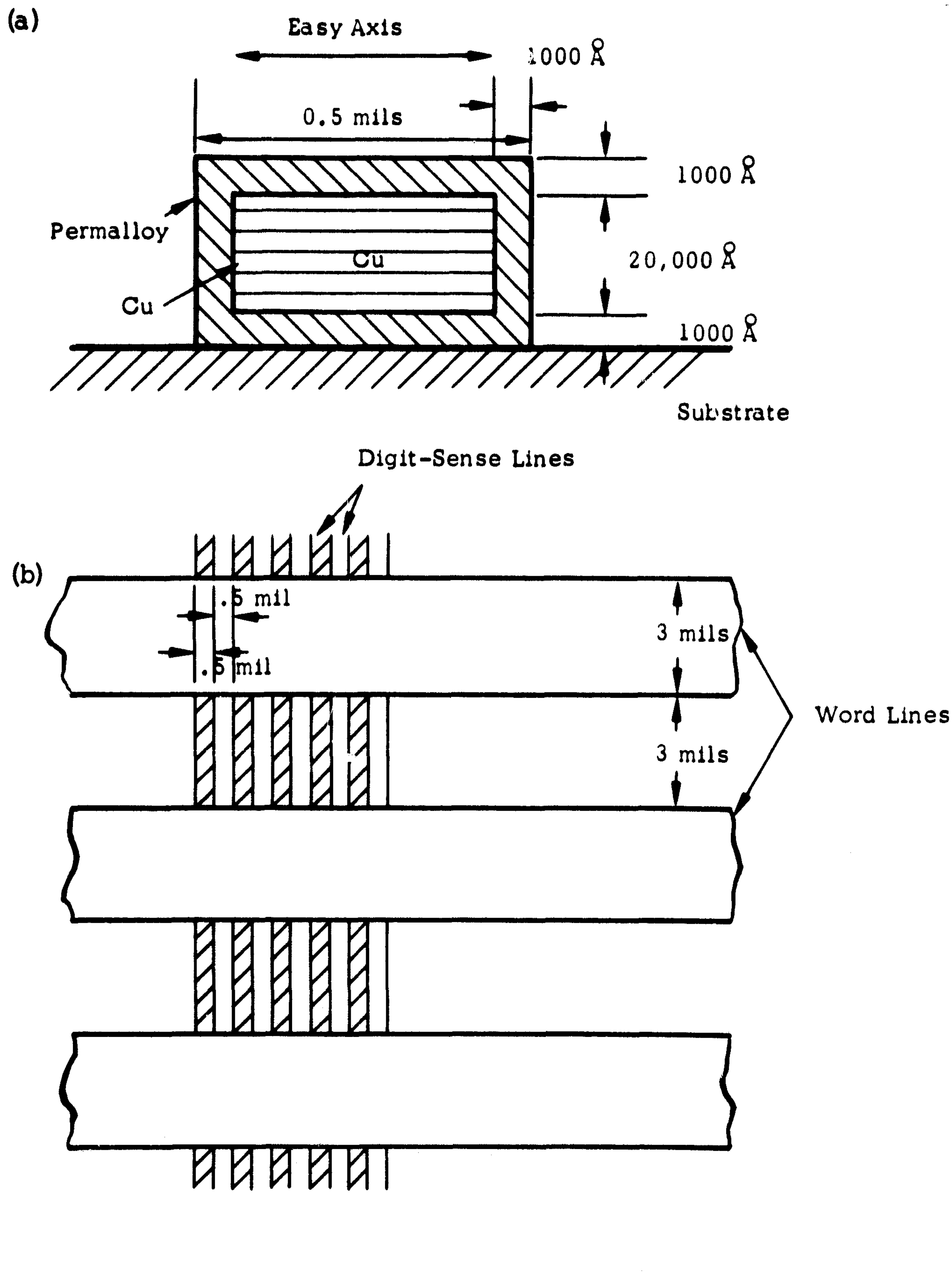

Fig. 5 High Density Memory Plane

3.0 OPERATION OF THE DEVICE

3.1 Storage Location

In a uniaxial thin film there are two stable minimum energy states for magnetic dipoles parallel to the easy axis. A region of parallel oriented magnetization is called a domain (Fig. 3). Information is stored in the thin films in the form of magnetic domains; the domain orientation indicates whether a zero or a one has been stored.

Two different orientations of the easy axis are conceivable: along the digit line -- called longitudinal easy axis -- or orthogonal to the line -- called circumferential easy axis.

3.1.1 Circumferential Easy Axis

Flux and domain are closed around the line in the quiescent state. During word drive (drive field perpendicular to easy axis) the closure is broken up and demagnetizing fields are generated. (Fig. 6a) Since the domains are very stable in this configuration they make a memory insensitive to external stray fields, but require relatively high word drive currents to overcome the demagnetization fields.

3.1.2 Longitudinal Easy Axis

In this case the flux is being closed during hard-axis drive and consequently requires less word current. A severe drawback of this configuration is the open flux of the domains in the absence of hard-axis drive making the domains susceptible to external fields (Fig. 6b).

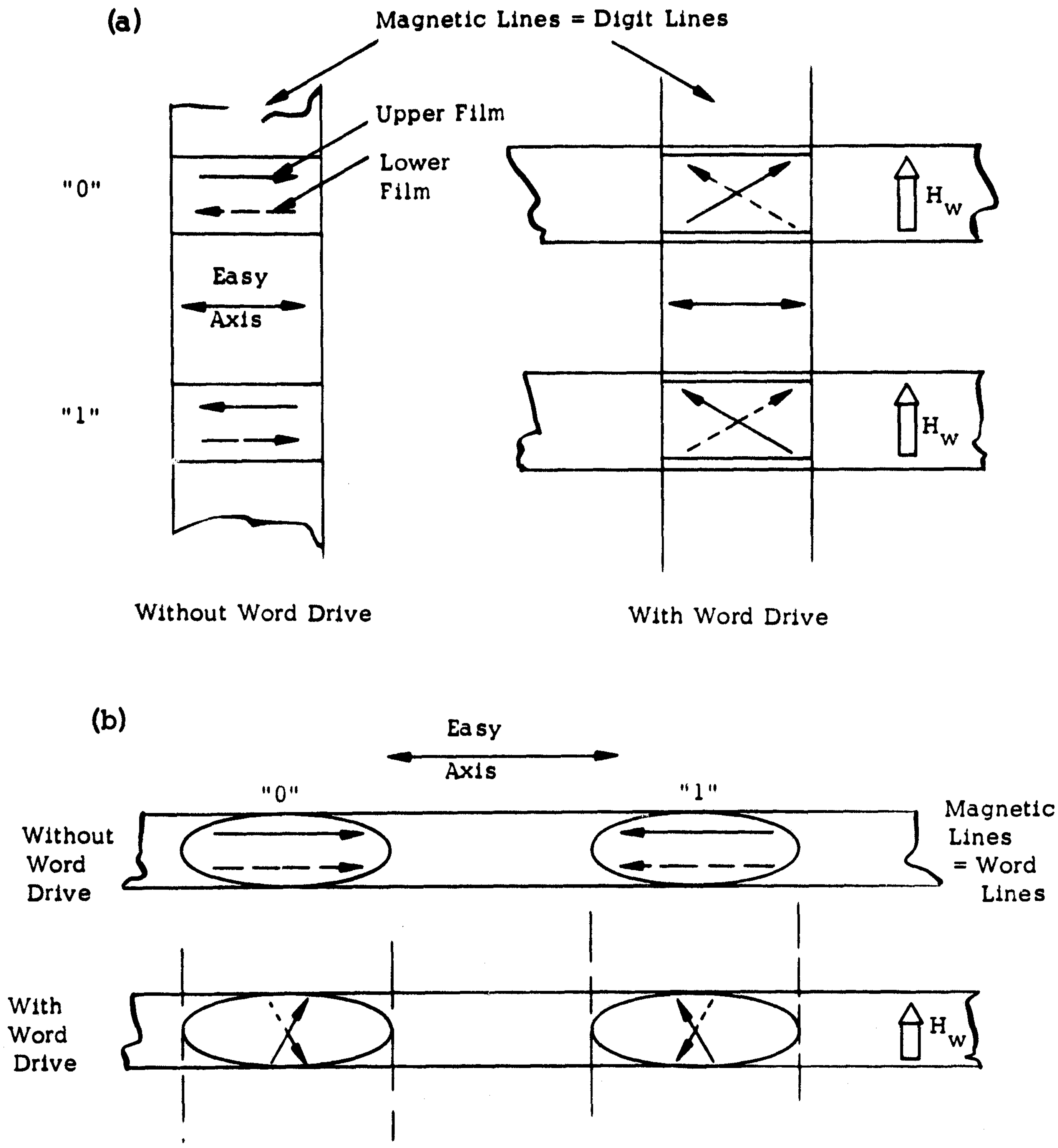

Fig. 6 Domains with Longitudinal and Circumferential Easy Axis

3.2 Write Operation

Simultaneous application of hard-axis and easy-axis drive nucleates a "0" or a "1" domain depending on the polarity of the easy-axis drive. The word current forces the magnetization into the hard (or transverse) direction. With the subsequently applied easy-axis field in the anisotropy dispersion is overcome and all the dipoles are forced to fall on one side (Fig. 7).

3.3 Read Operation

Only a hard-axis field is applied to the domain. The closed flux around the digit line is broken up and disappears as soon as the magnetization is driven fully into the transverse direction. This flux change induces a sense voltage in the digit line with a polarity depending on the information stored in the domain (e.g. "0" domain induces positive, "1" domain negative sense signal).

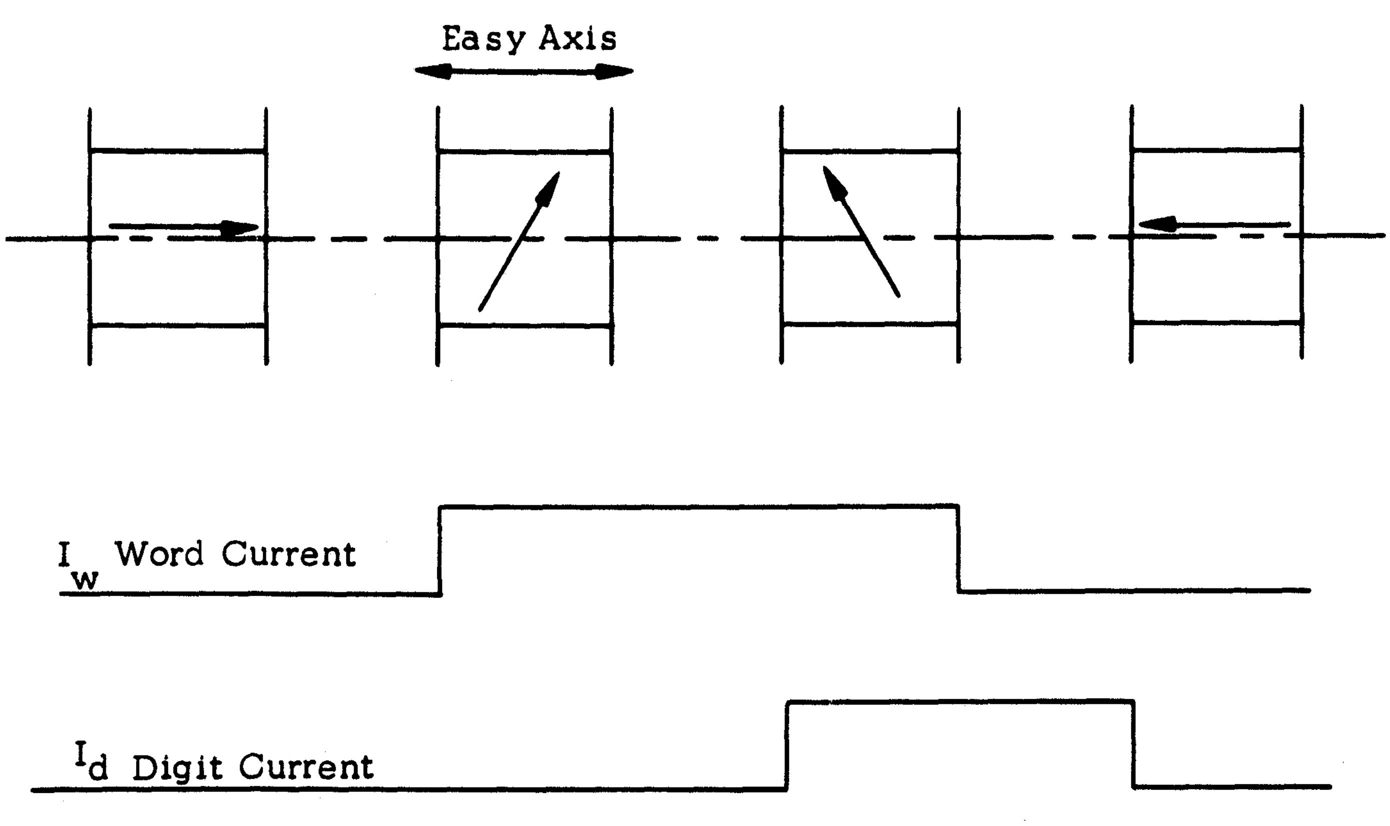

Fig. 7 Write Operation

The amplitude of the sense signal is determined by the total flux of one domain and the switching time. Flux, ϕ_o, and hence sense signal, V_s, are proportional to domain width ($2x_o$) and film thickness T.

$$V_s \sim \frac{\phi_o}{\Delta t} \; ; \; \phi_o = 2x_o \cdot T \cdot M_s$$

M_s = saturation moment.

Thus the sense signal depends on the width of the word drive line but does not depend on the width of the digit line (magnetic line), implying that the density of the digit line can be increased without any loss in sense signal.

4.0 DEMAGNETIZATION EFFECTS

Unclosed flux is present in the case of the circumferential easy axis during hard axis drive, and in the case of longitudinal easy axis during absence of transverse drive. The demagnetization fields due to the open flux lead in the first case to higher drive requirements and in the second case to unstable domains unless the coercive force of the film is considerably higher than the demagnetizing fields.

4.1 Longitudinal Easy Axis

We assume the domains to be of elliptical shape, in which case the demagnetization factors N are known [1] (Fig. 8).

The demagnetization field H_d is well know to be:

$H_d = 4\pi N M_s$; $M_s = 800$ oe for permalloy

Since both layers of film are switched in the same direction both contribute to the demagnetization field; for a 1000Å film, therefore, the effective thickness is 2000Å. For a domain width b = 1/2 mil and a domain length, a, following demagnetizing fields are obtained (T = 1000Å):

a =	H_d
3 mils	10 oe
6 mils	3.4 oe
8 mils	1.8 oe

H_c, the coercive force, has to be larger than H_d, and since H_c is approximately 2 oe (Sec. 8.0) 8 mils is the minimum length for stable domains.

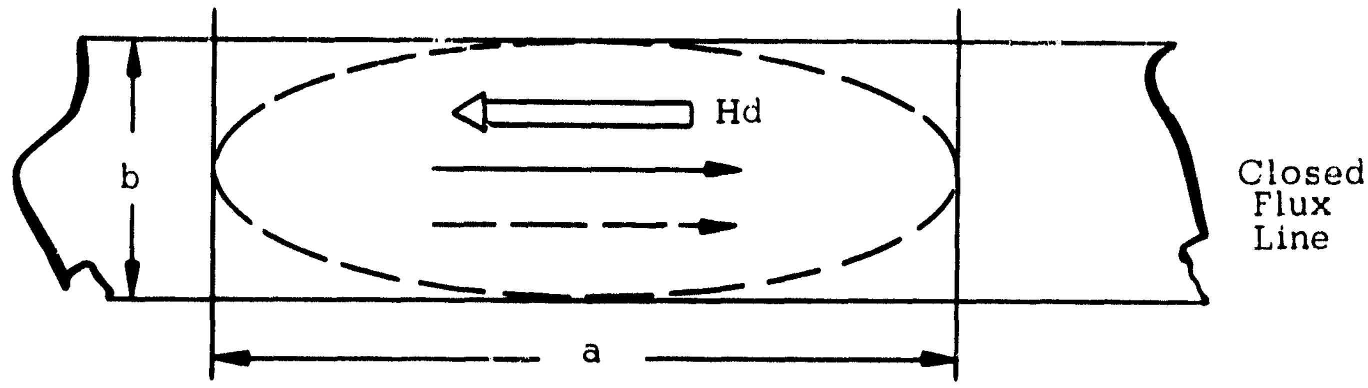

Fig. 8 Demagnetization Longitudinal Easy Axis

4.2 Circumferential Easy Axis

During word drive the magnetization is rotated toward the transverse direction. The angle of rotation and hence the hard axis component of the magnetization depend on the applied drive field and the location within the digit line. (See Fig. 9.) This demagnetization problem leads to an integral equation which is treated in Appendix I. Figure 10 shows magnetization distributions for different parameter values K and an applied field $h_a(x)$ being a unit step function of x:

$$h_a(x) = 1 \quad |x| \leq x_o$$
$$h_a(x) = 0 \quad |x| > x_o$$

$$h_a(x) = \frac{\text{applied field}}{H_k} \qquad K = \frac{2 \cdot T_{eff} \cdot M_s}{H_k \cdot x_o}$$

$T_{eff} = 2T$; H_k = anisotropy field (≈4.5 oe)

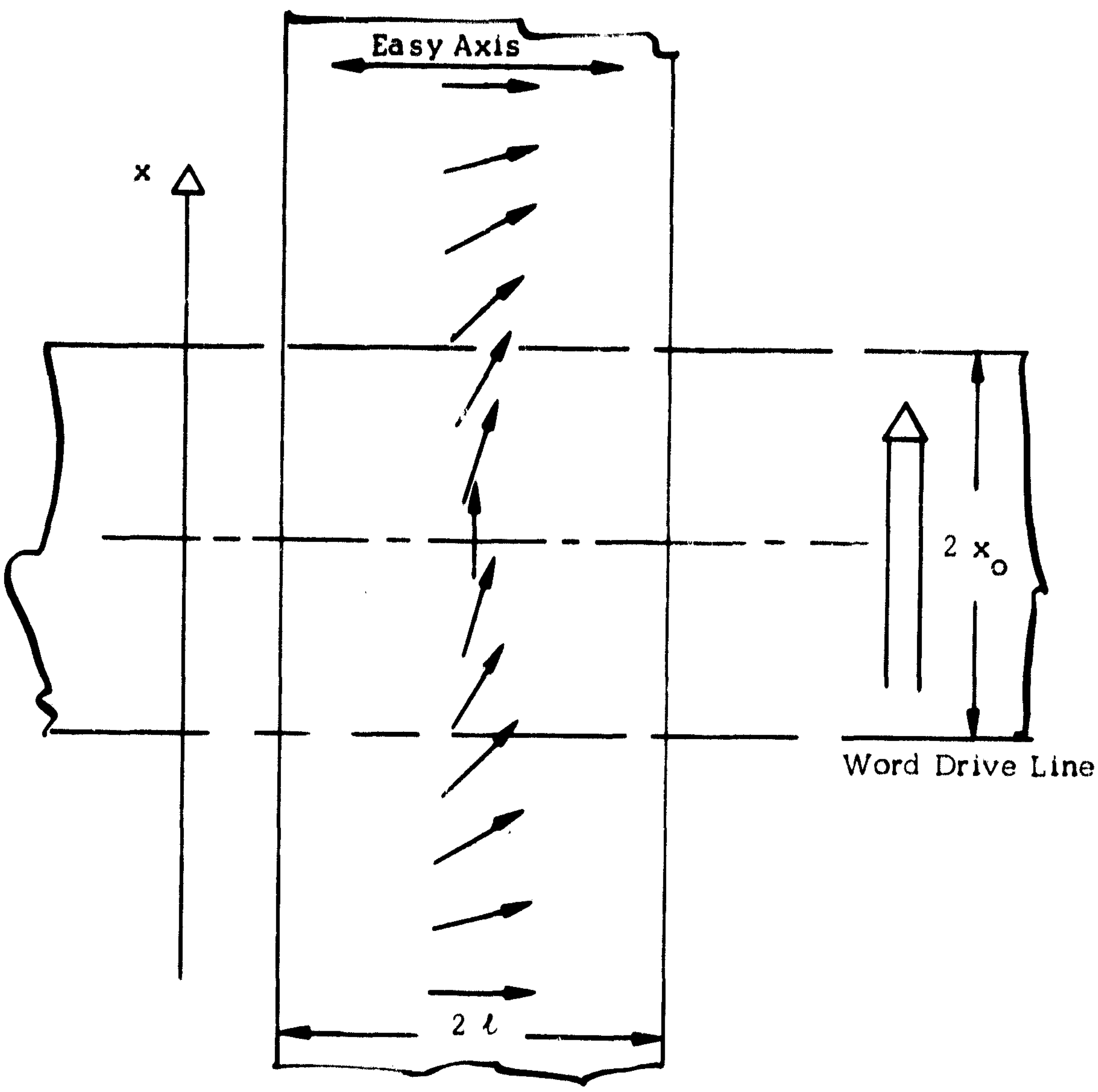

Fig. 9 Demagnetization Circumferential Easy Axis

2L is the width of the digit line normalized with respect to x_o. K has the meaning of a field shape parameter. The bigger K, the smaller the total field (applied field - demagnetizing field) and the more the magnetization distribution is spreading along the digit line, making high word density impossible.

Fig. 10 includes the distributions for the following choices of parameters (digit line width = .5 mil)

Drive line width $2x_o$	Film Thickness	K	L
1 mil	1000 Å	5.3	.5
3 mils	1000 Å	1.8	.17
2 mils	500 Å	1.35	.25

(The last two sets of parameters give almost identical magnetization distributions.)

It is readily seen that 1 mil wide drive lines give ill-defined total field distributions within a 1000Å film. Three mil wide drive lines and 3 mil gaps for 1000Å films, and 2 mil wide drive lines and 2 mil gaps for 500Å films are adequate, allowing a word density of 166 and 250 words per inch respectively. Since there are 1000 digit lines to the inch the following storage densities are feasible:

1000Å film: 166,000 bits/inch^2

500Å film: 250,000 bits/inch^2

In a two-spots-per-bit configuration, which probably has to be chosen for noise cancellation (see Appendix III), the above density figures have to be divided by two.

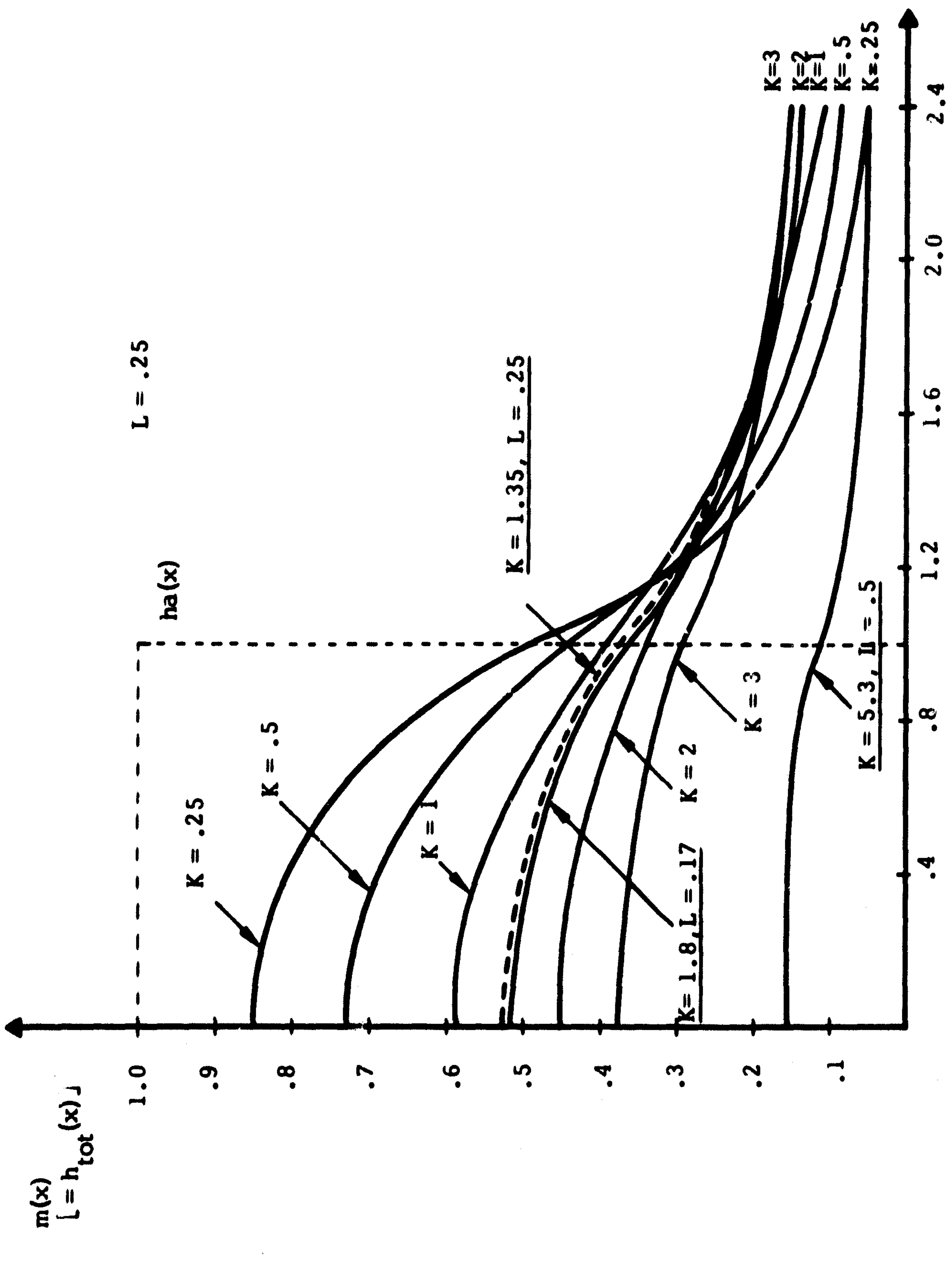

Fig. 10 Magnetization Distribution

5.0 DRIVE REQUIREMENTS

Since the circumferential easy axis was proved to be the more promising configuration we only specify drive requirements for this case. As was pointed out in Chapter 3, the word current has to drive the magnetization into the hard axis; the digit current essentially has to be high enough to overcome anisotropy dispersion.

Close to the drive lines the produced fields are proportional to the current and inversely proportional to the drive line width. For the digit line (.5 mil wide) $H_D = .48 * I_D \text{(Oe)}$

$$H_w = .08 * I_w \text{(Oe)}$$

Fig. 10 shows that for K = 1.8 and an applied field equal to the anisotropy field H_k, the total field in the center of the strip line is only about $H_k/2$; hence to drive the magnetization fully into the transverse direction the applied field has to be at least twice the anisotropy field:

$$H_w \approx 2\ H_k$$

which requires a drive current

$$I_w \approx 25 * H_k \cong 110 \text{ mA for } H_k = 4.5 \text{ Oe}$$

The easy axis field has to be smaller than H_c; otherwise digit disturb pulses would wipe the information out.

$$H_D < H_c; \quad H_c \cong 2 \text{ oe}$$

providing a limit for the digit current:

$$I_D < 5 \text{ mA}$$

6.0 ELECTRONIC TESTING

Two sensing methods have been investigated:

1) R. F. sensing
2) Wideband sensing

Where the feasibility of the R. F. sensing was proven, the wideband sensing was actually used to evaluate the memory planes.

6.1 R. F. Readout

A domain is exposed to an R. F. hard-axis drive. This drive causes the magnetization to oscillate between the positive and negative hard axis. For a full period of the drive field the flux changes twice from its maximum to its minimum, generating a sense signal of twice the frequency of the R. F. drive (see Fig. 11). The phase of the sense signal depends on the orientation of the domain being interrogated: e. g., 0-phase indicates a "0" domain, 180° phase a "1" domain (see Fig. 12). R. F. sensing allows the application of narrowband (tuned) amplification leading to good S/N ratios. Information is read out using phase detection.

Experiment:

A 20 MHz hard-axis drive was applied to the 10 mil memory lines. The sense signal was passed through a 40 MHz narrowband filter and displayed on the oscilloscope. Figure 13 shows the applied drive field and the obtained sense signal for both a "0" and a "1" domain. The 180° phase shift is evident from the picture. The measured sense amplitudes are consistent with expected values. (See Appendix II.)

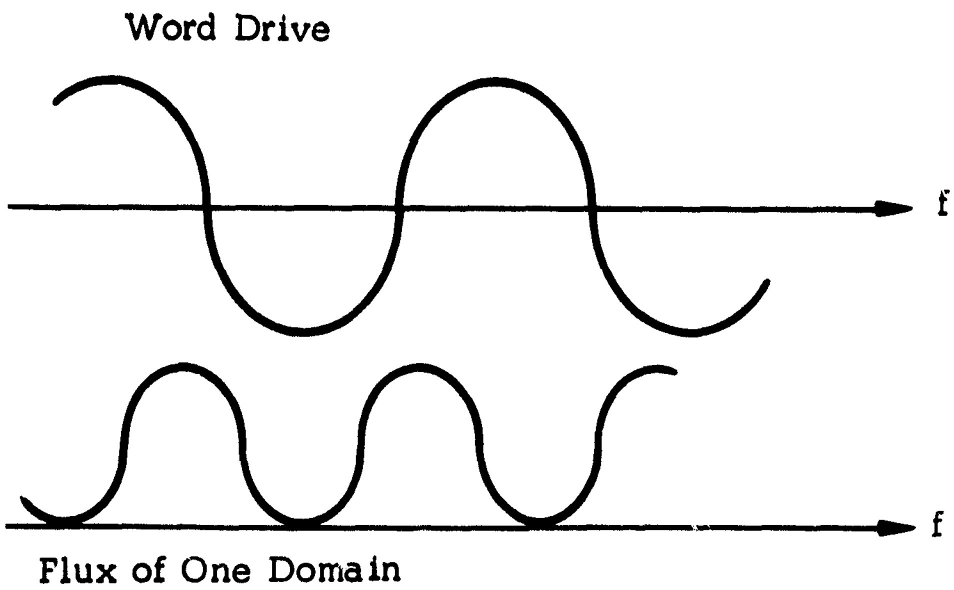

Fig. 11 Frequency Doubling in Pf Readout

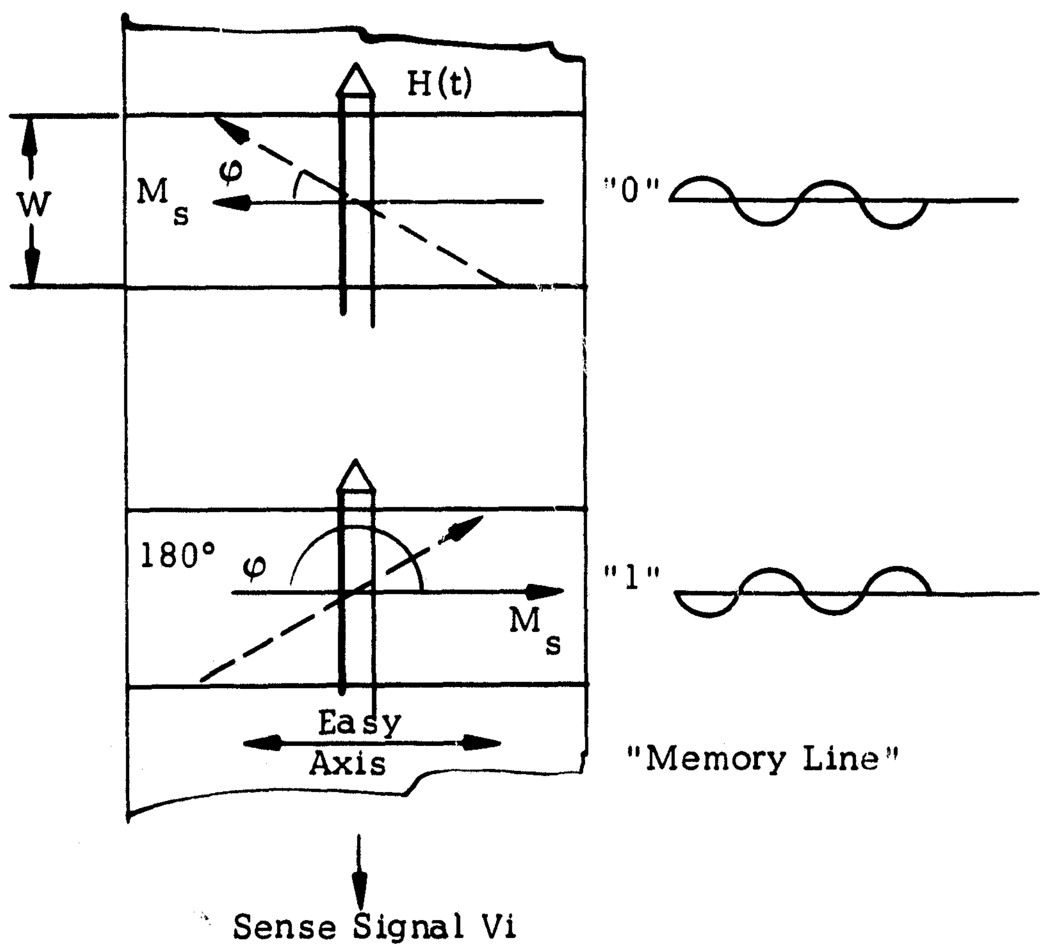

Fig. 12 Phase in R. F. Sensing

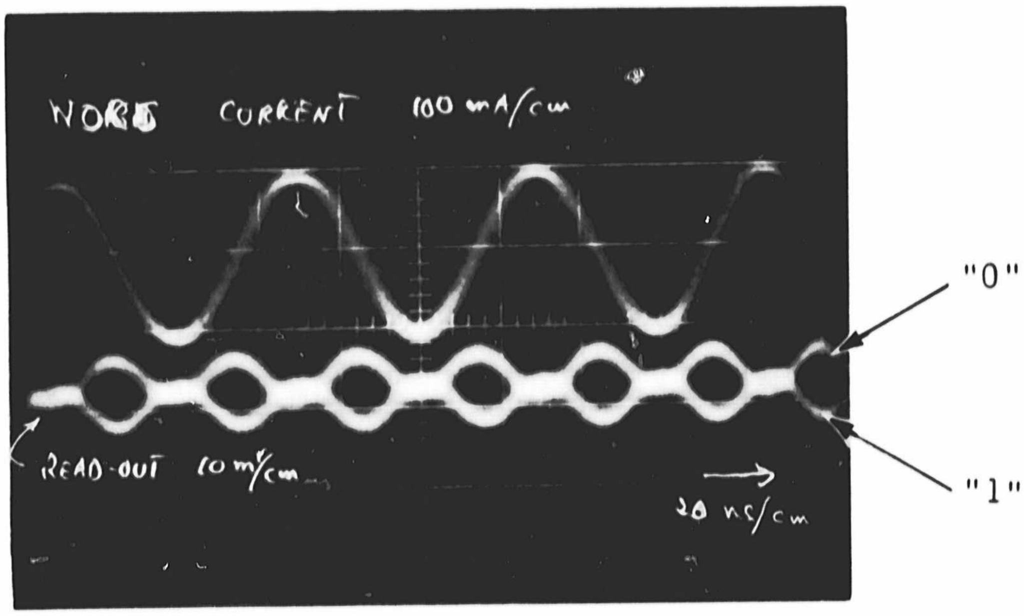

Fig. 13 Hard-Axis Drive and Sense Signals for "0" and "1"

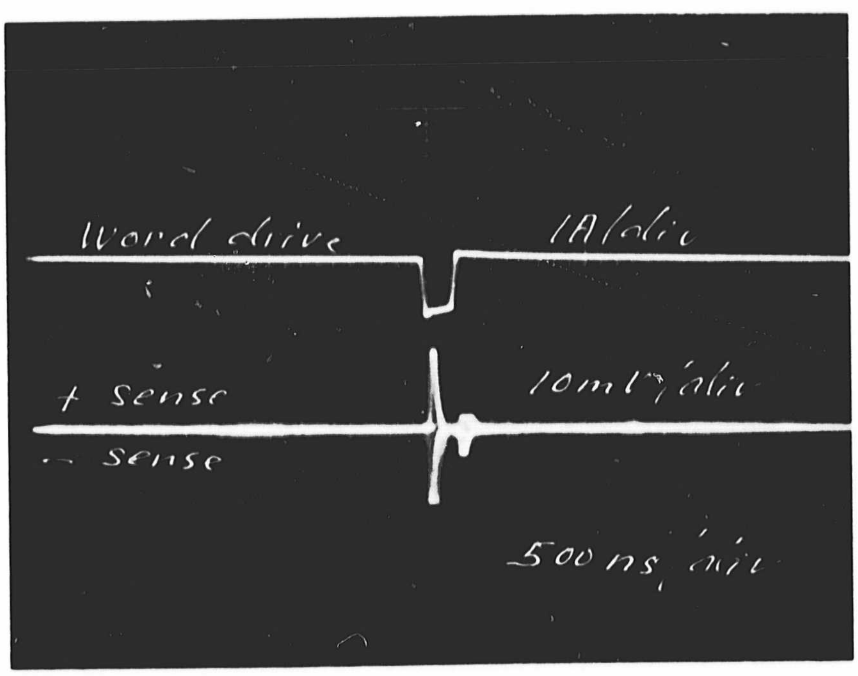

Fig. 14 Sense Signal (pos. peak: signal for "1", neg. peak: signal for "0") (2500Å thick film, 10 mils wide drive lines)

6.2 Wideband Readout

With the fast transition of a word current pulse, the magnetization of a domain is driven from the easy into the hard direction, changing the flux from its maximum value to zero, inducting a voltage "spike" in the sense lines. The polarity of the sense signal indicates whether a "0" or a "1" was stored in the domain. Figure 14 shows the drive pulse together with "0" and "1" signal. A two-spot-per-bit scheme was implemented to enable rejection of common-mode noise by a differential amplifier connected to both sense lines. Due to a bridge configuration the inputs to the sense amplifiers are virtually kept at ground during digit drive, which cuts down considerably the recovery time of the digit system (see Fig. 15).

6.3 Test Program

Worst case testing was used to evaluate the memory planes. The information is written only once against a domain saturated in the opposite direction. After writing, the bit is exposed to 256 disturbs and then read out. The full test sequence is shown in Fig. 16. Details of drive and sense electrons are found in Appendix III.

6.4 Test Results of 10 Mil Memory Lines

Because of the connection problem with the high density memory planes most of the electronic tests were carried out first on a larger scale with 10 mil wide digit lines and 15 to 20 mil word lines. Film thickness and word line width were chosen to achieve similar demagnetization conditions to the high density plans. Results gained from the large memory elements will thus be conclusive for the small ones too. Figure 17 shows the sense signal versus digit current I_D for a 2500Å thick magnetic film. Since the wider digit lines give rise to higher demagnetizing fields during word drive, an additional film was put on top of the word lines to compensate part of the

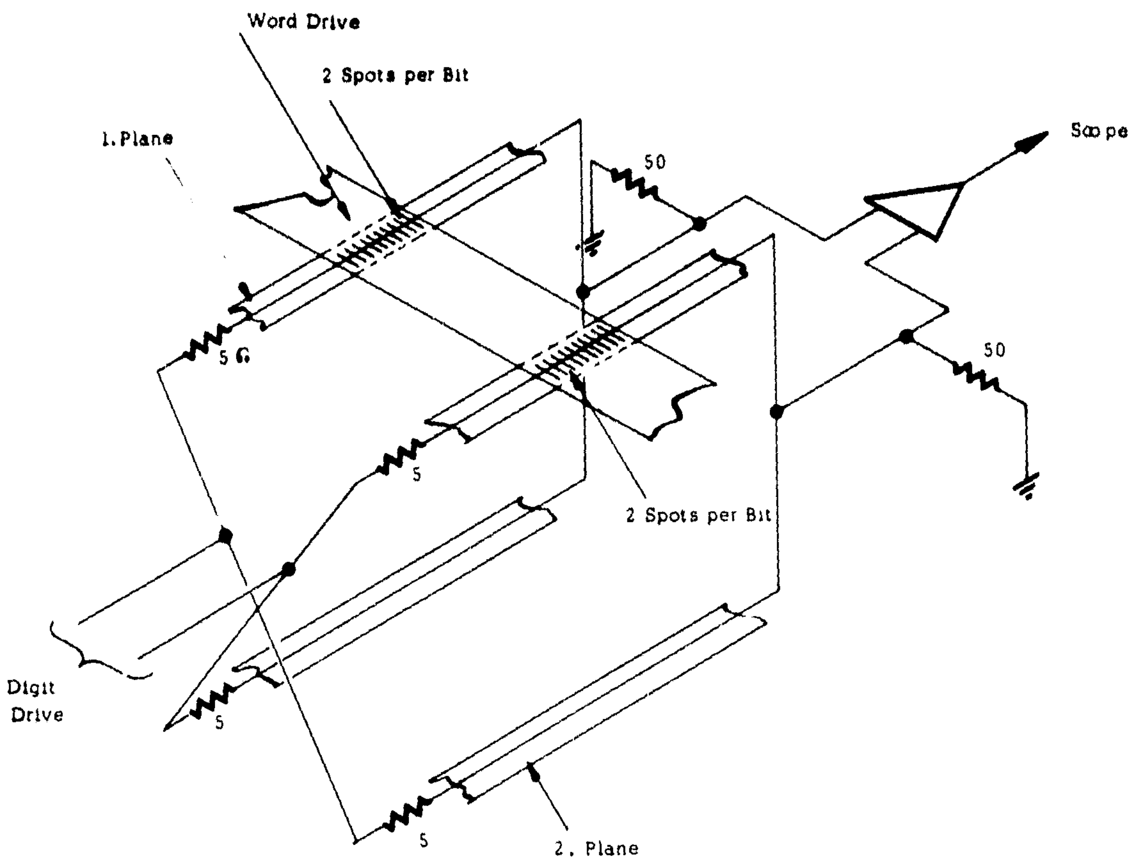

Fig. 15 Bridge Configuration

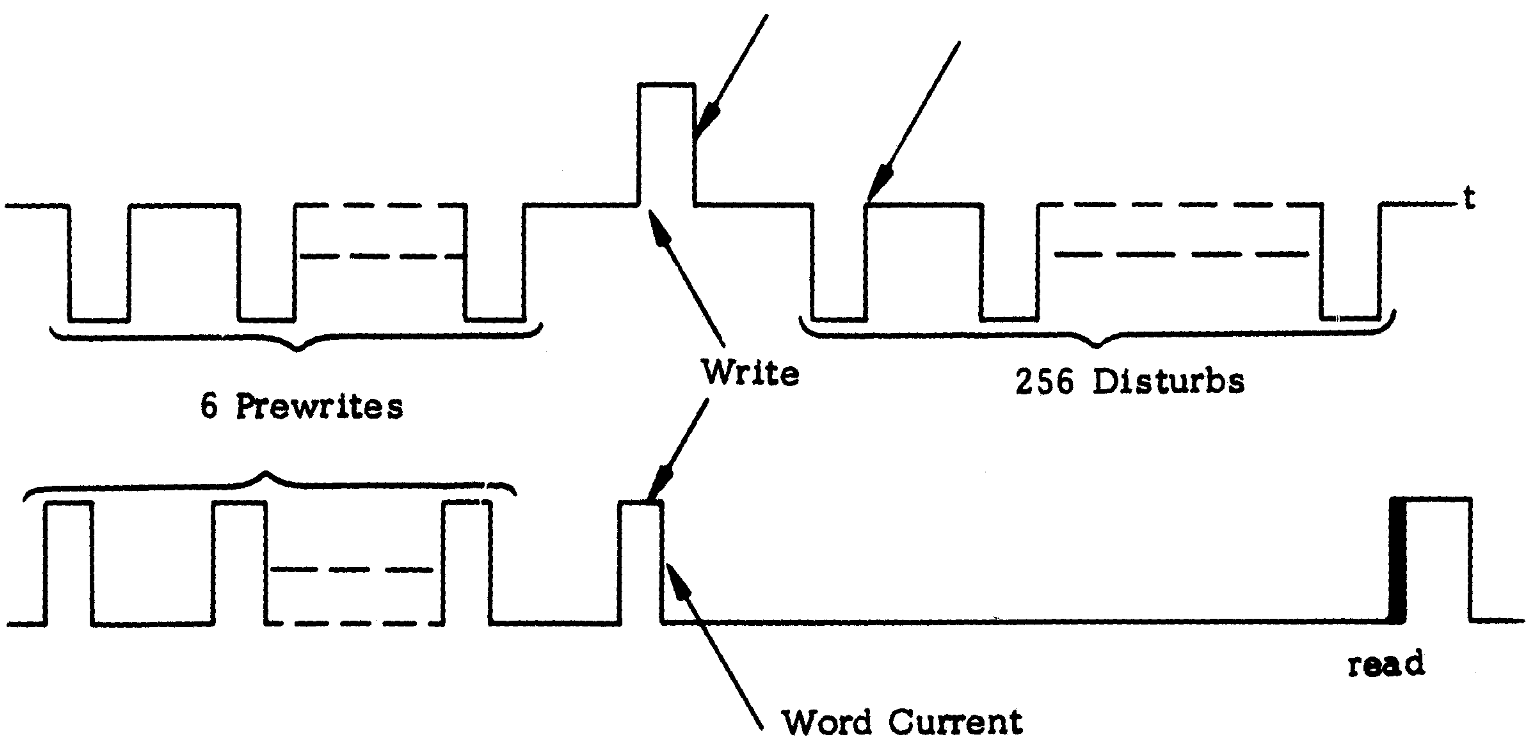

Fig. 16. Test Program for Worst Case Testing

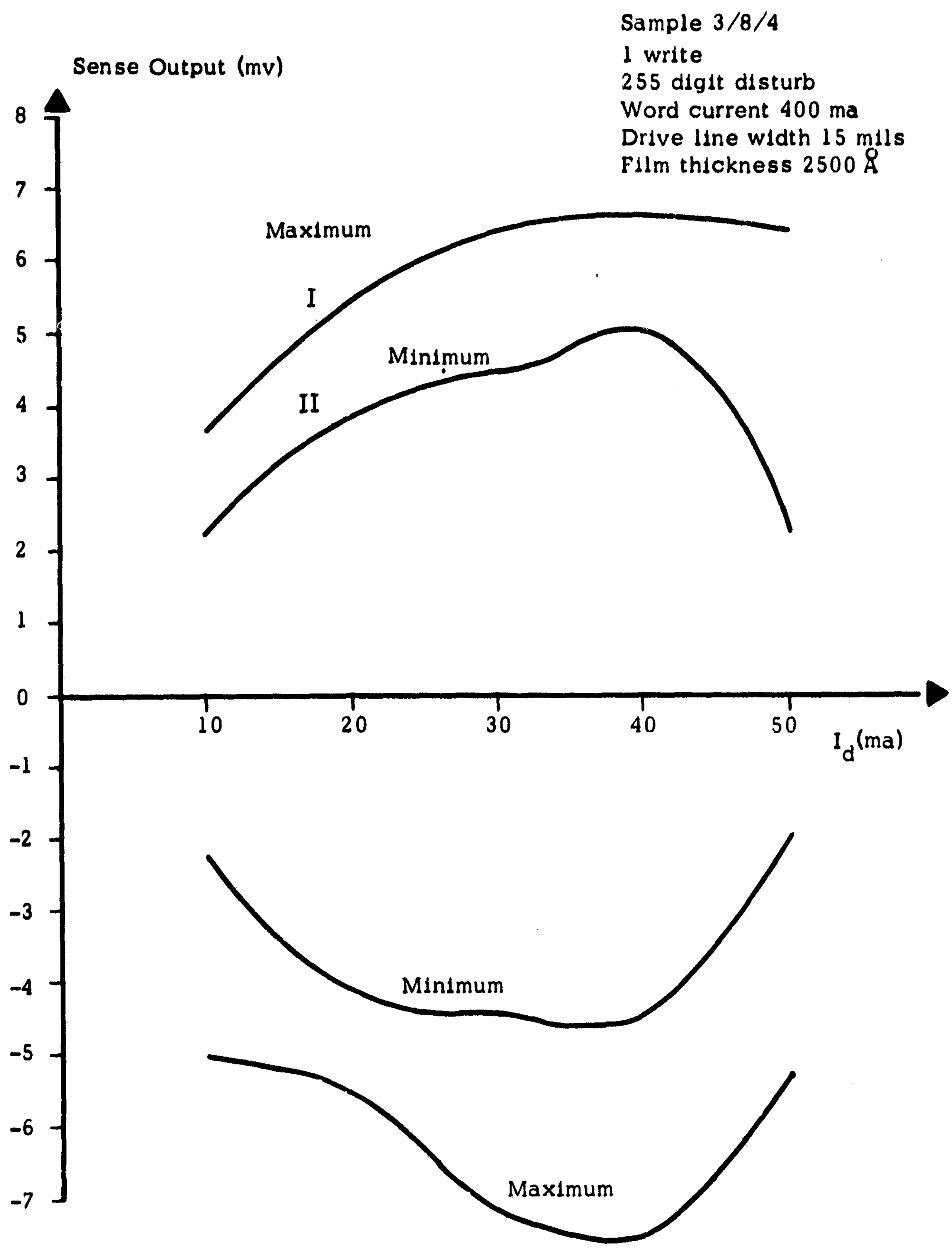

Fig. 17 Sense Output Versus Digit Current

higher demagnetization fields (see Appendix I). Curves 1 and 2 give maximum and minimum signals gained from 256 bits distributed over the 1" x 1" memory plane. Figure 18 gives a trace of the peak-to-peak signal as a function of the word current for optimum digit drive. With the help of this curve an economical word drive can be decided upon. At 400 mA word current we recognize a break in the curve: to go higher in current brings little in sense signal but makes drive requirements much more stringent.

Consistency of the magnetic film throughout a 1" x 1" plane has been proven. Operational margins under worst case testing look good for all tested bits. A workable memory plane has been obtained.

6.5 Feasibility of NDRO

It has been found that the films tested with destructure readout (DRO) also perform well in nondestructive readout (NDRO) with equal read-write word current. A special layer of hard magnetic material would require higher write than read drive, making the drive electronics much more complex and ruling out the possibility of a 2-1/2 memory organization.

For equal read-write NDRO mode the optimum digit current is approximately twice the current for DRO but only half the word current is required. Sense signals in NDRO are approximately one third of those obtained with DRO.

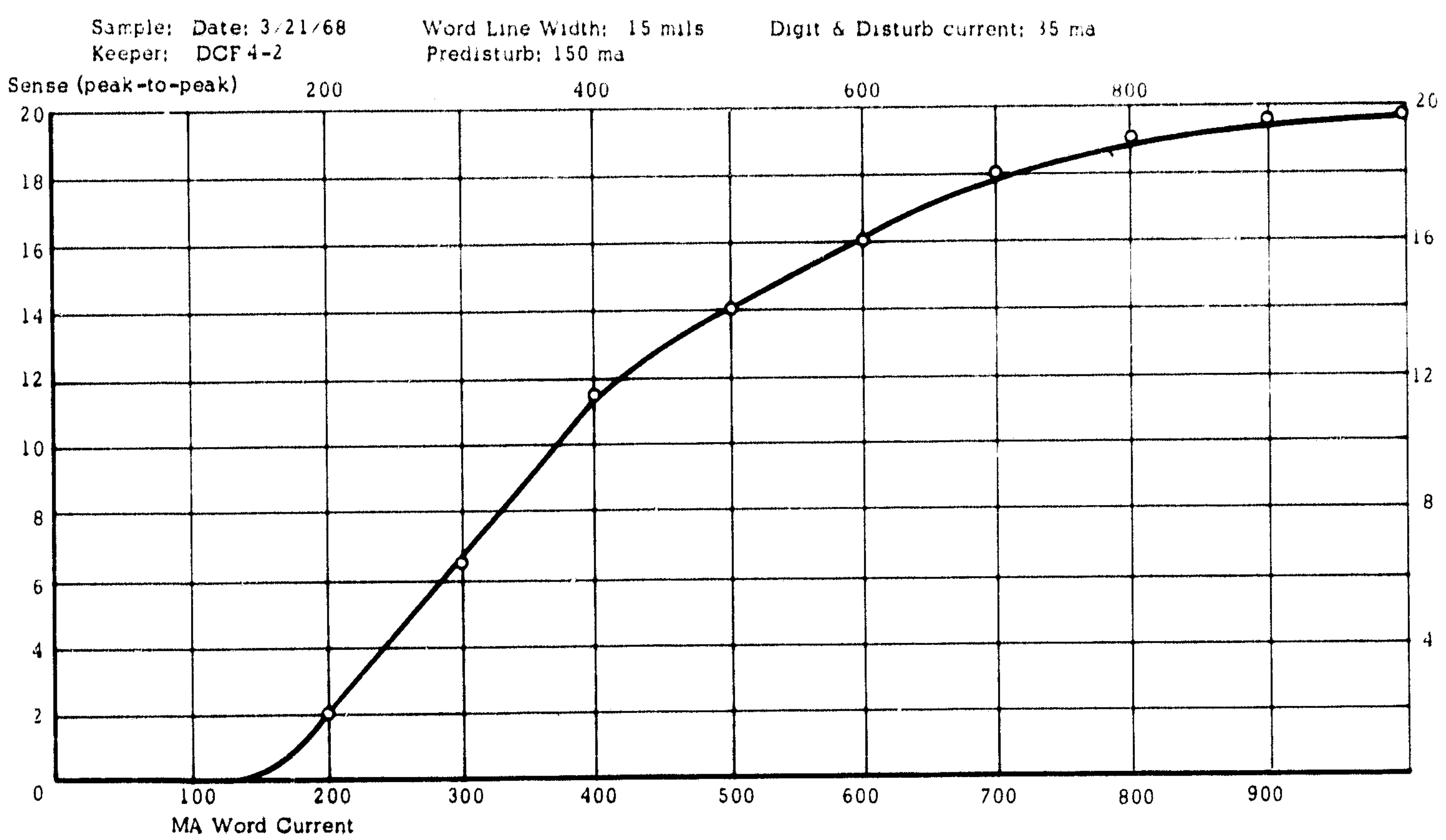

Fig. 18 Sense Signal Versus Word Current

PART II: FABRICATION OF THE MEMORY PLANES

PRECEDING PAGE BLANK NOT FILMED.

7.0 GENERAL PROCEDURE

Due to the availability of substrates, all samples have been prepared using glass slides 1" x 1" (cover slips Corning #1-1/2), except for one sample which was plated on silicon to prove the feasibility of silicon as a substrate. The individual layers deposited are shown on a somewhat distorted scale in Fig. 19a.

A NiCr layer is first sputtered onto the glass to provide good adhesion to the substrate. Subsequently, a copper layer is evaporated on top of it which provides a conductive but inert surface. All subsequent metallic layers are applied by electroplating techniques. First a Permalloy layer is deposited. Next comes a heavy deposition of copper, which later will be used as a conductor. The final Permalloy layer follows on top of the copper. Special care was taken to provide identical properties for both magnetic layers. Using photoresist techniques, the entire memory plane is then etched into individual memory lines.

The final cross section of the simple sandwich is shown in Fig. 19a. Note that the edges in this picture, the scale of which is distorted, are not cut vertically because the etching process is not perfect. Due to this slant, the individual layers become exposed and can be observed microscopically (Fig. 20a). After all unwanted material has been etched away totally from the glass substrates, the simple sandwich may be supplemented by an additional layer of magnetic material which closes the gap between the first two layers as shown in Fig. 19b. This last layer is obtained by an additional permalloy plating step while photoresist still covers the planar part of the magnetic line. The microscopic picture of an edge where the flux closure layer has been applied is demonstrated in Fig. 20b. Note that the closing layer appears much more grainy than the planar magnetic film.

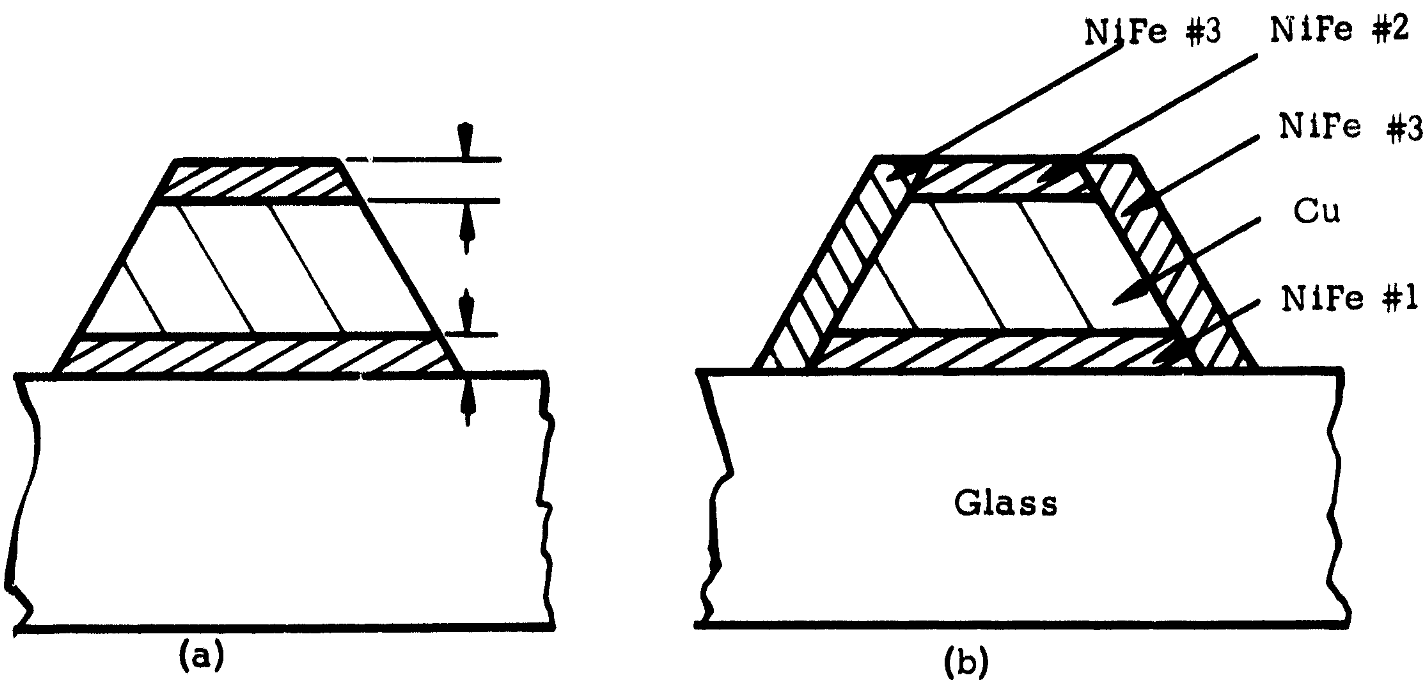

Fig. 19 Cross-Section of Memory Lines

(a) Simple Sandwich

(b) Closed Flux Structure ("Plated Wire Analogue)

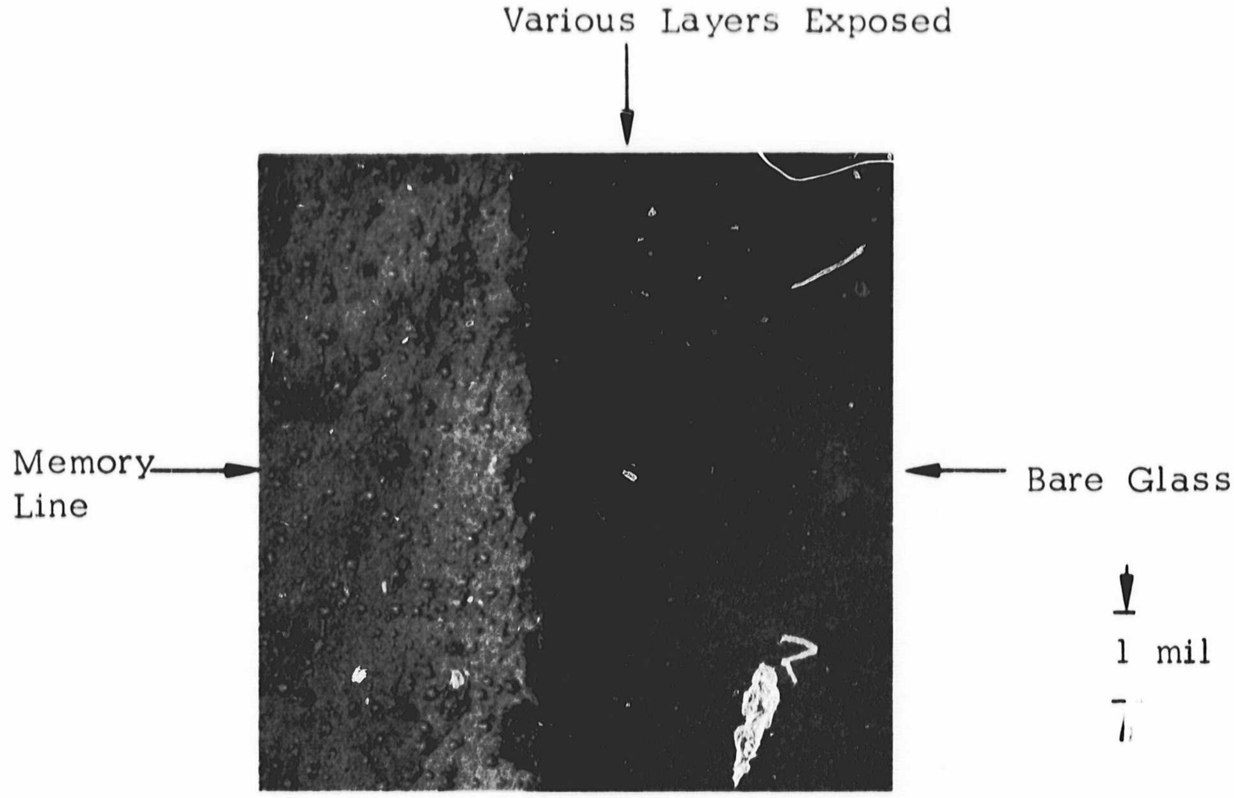

(a)

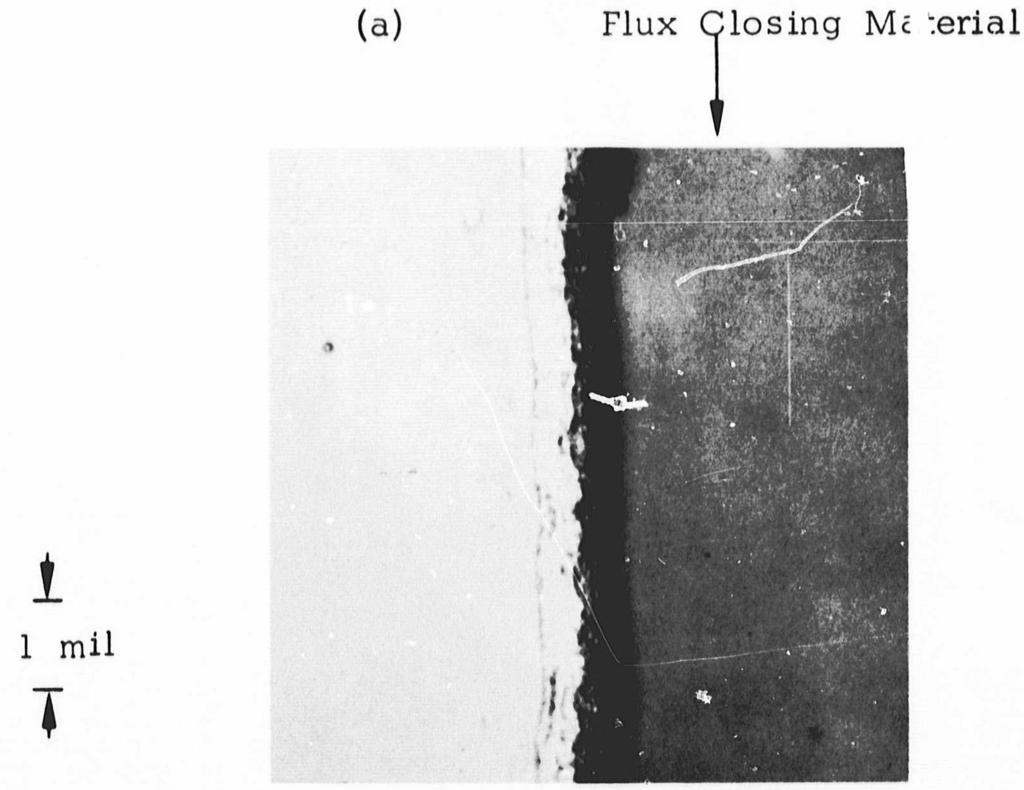

Fig. 20 Microscopic Observation of Edge of Sandwich Structure

(a) Simple Sandwich; Individual Layers Exposed
Sample # 7-3-6, 30 mil Lines

(b) Closed Flux Structure;
Sample # 4-7-1, 30 mil Lines

PRECEDING PAGE BLANK NOT FILMED.

8.0 BULK MAGNETIC TESTING

After all layers have been deposited on the 1" × 1" substrate (2 NiFe + Cu layer) both the easy and the hard axis M-H loops of the sample are traced. From these curves the following film parameters are determined:

H_c: coercive force
H_k: anisotropy field
H_s: saturation field

Figures 21 a and b show the loops for a typical 1000Å sandwich structure. We read:

$$H_c = 2 \text{ Oe}, \; H_s = 3 \text{ Oe}, \; H_k = 4.0 \text{ Oe}$$

To measure the anisotropy dispersion an ac hard axis field and a dc easy axis field are applied simultaneously. First the peak signal is determined for 100% switching, then the dc field is lowered until 90% of the magnetization is being switched. From this dc field and H_k the dispersion is easily computed. Figure 21 c shows the "100% curve" and the 90% curve. The dispersion is $\alpha_{90} \approx 2.5°$.

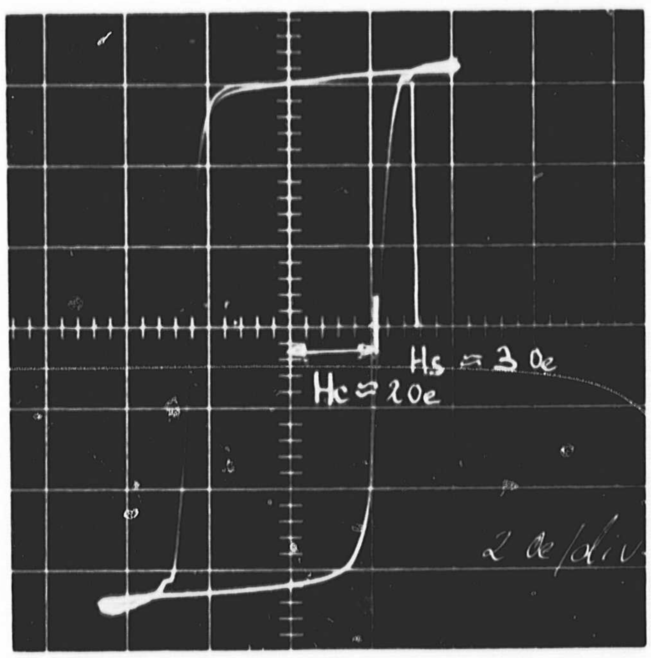

(a)

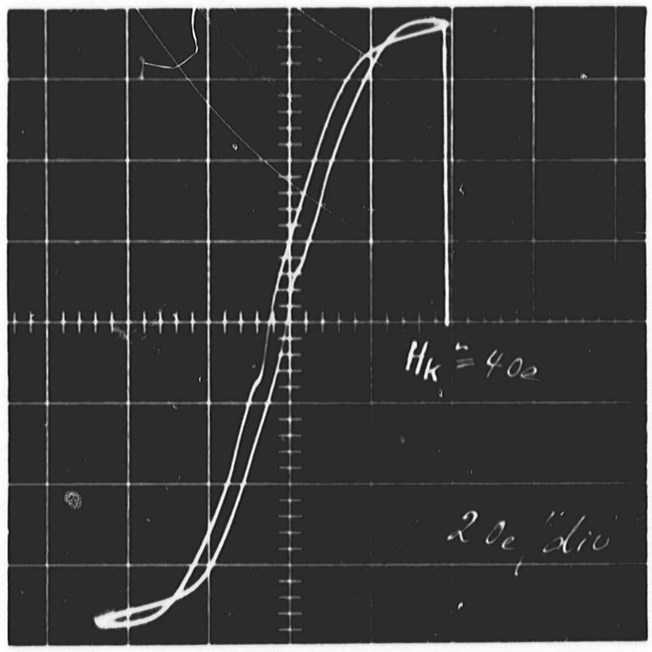

(b)

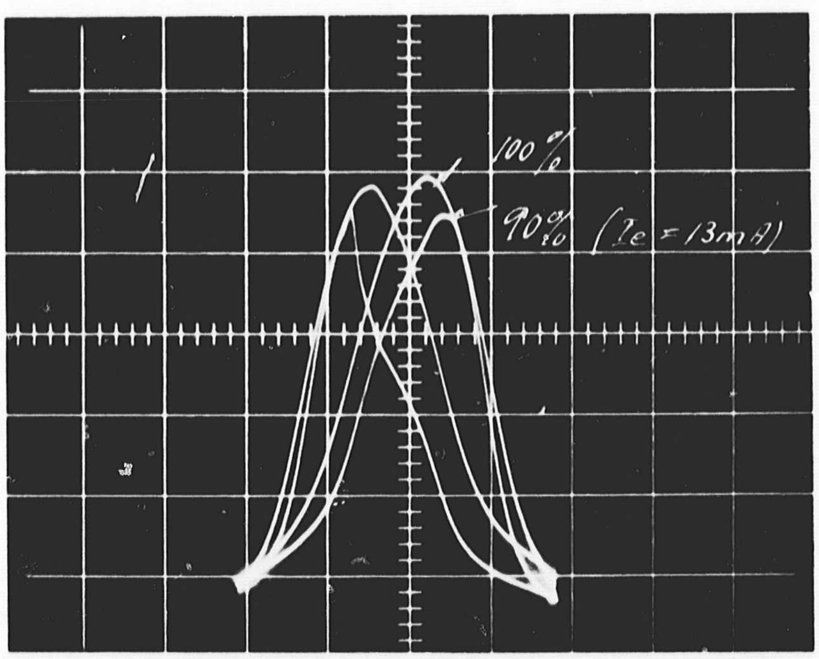

(c)

Fig. 21 Bulk Magnetic Testing

(a) Easy Axis Loop, (b) Hard Axis Loop,

(c) 100% and 90% Loops for Dispersion Measurements

9.0 PHOTORESIST AND ETCHING PROCEDURE

Since the digit line density is limited only by the technology to etch very fine lines out of the sandwich structure a detailed outline of the photoresist and etching procedure is given.

Procedure

Cleaning:

1) Clean samples in a clean bench (detergent wash, rinse in distilled water).
2) Degrease samples in degreaser 10 min.
3) Dry at 100° F for 10 min.

Photoresist Process:

4) Apply photo resist using eye dropper.

   Composition of photo resist:

   3 parts KMER

   1 part KMER thinner

   Centrifuge for 12 hours at 4550 rpm.

   Pour or siphon off clear liquid for use.

   Note: This solution good only for one week. After elapsed time, respin for 8 hours.

5) Spin coat as follows:

   3000 rpm for 10 sec.

   4000 rpm for 5 sec., depending upon surface produced.

   Note: Wet sample completely before starting spinner.

6) Air dry for at least 75 min.

7) Bake at 185° F for 5-10 min. (not longer than 10 min.)

8) Expose 2 - 3 min, sample and mask have to be in intimate contact

9) Develop 2 - 3 min. in KMER developer

10) Rinse with Stoddard solvent spray.

11) Rinse with lukewarm water.

12) Air dry

13) Post-bake at 280° F for 120 minutes

Etching:

14) Electro etch for 60 sec at current density 25 mA/in^2.
Bath composition:
10% HNO_3, distilled water, sodium laurel sulphate 4 grams/ liter, room temp. 72° F. (If edge definition breaks down, renew bath.)

15) Chemical etch by dipping.
Bath composition:
42% nitric acid solution and distilled water at 40° C.
Dip until glass substrate shows clear between lines.

16) Determine etch-factor, and line width.

17) Evaporate 200Å of SiO before flux closure.

18) Reactivate line edges by dipping into 5% HNO_3 and distilled water solution for 25 - 30 sec.

With this procedure lines from 10 mils down to 1/4 mil width have been successfully etched. Figures 22 to 24 give pictures of memory planes with line densities ranging from 50 lines per inch to 1000 lines per inch.

Pictures 25 - 27 show the facilities for evaporation, plating, and photomasking.

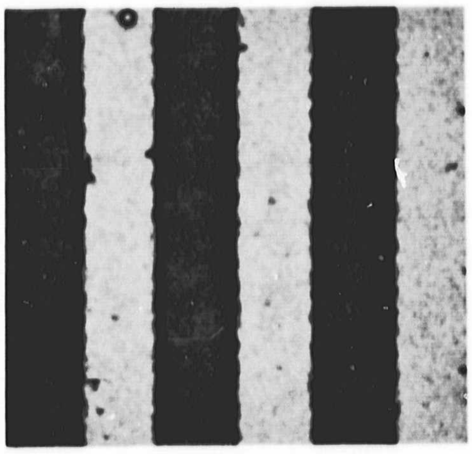

20 Mils
Center to Center

6 Mils
Center to Center

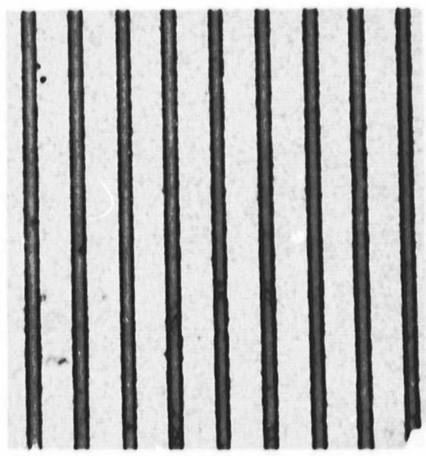

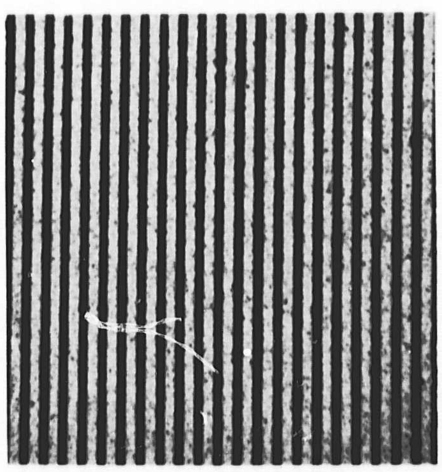

2 Mils
Center to Center

Fig. 22 Section of 10 Mil, 3 Mil and 1 Mil Wide Memory Lines (Reflected Light)

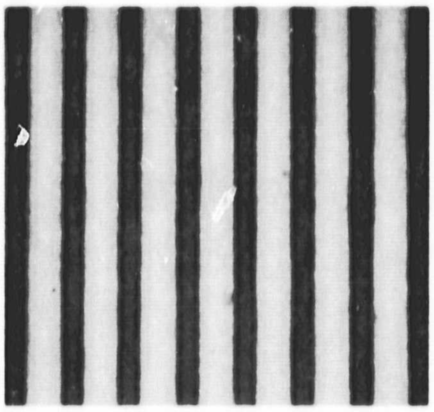

1 Mil Center to Center
(Reflected Light)

1 Mil Center to Center
(Transparent Light)

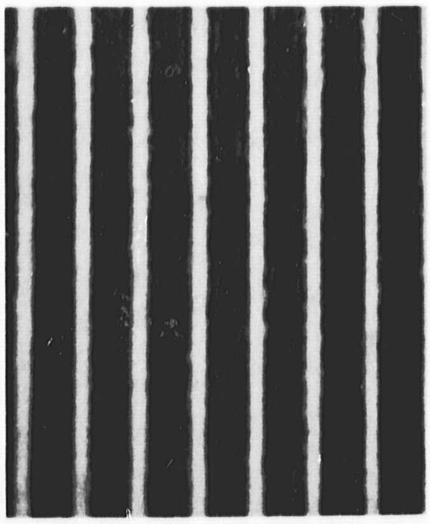

1 Mil Center to Center, 1/4 Mil Wide
(Reflected Light)

Fig. 23 Sections of 1/2 Line and 1/4 Line Wide Memory Lines

(a)

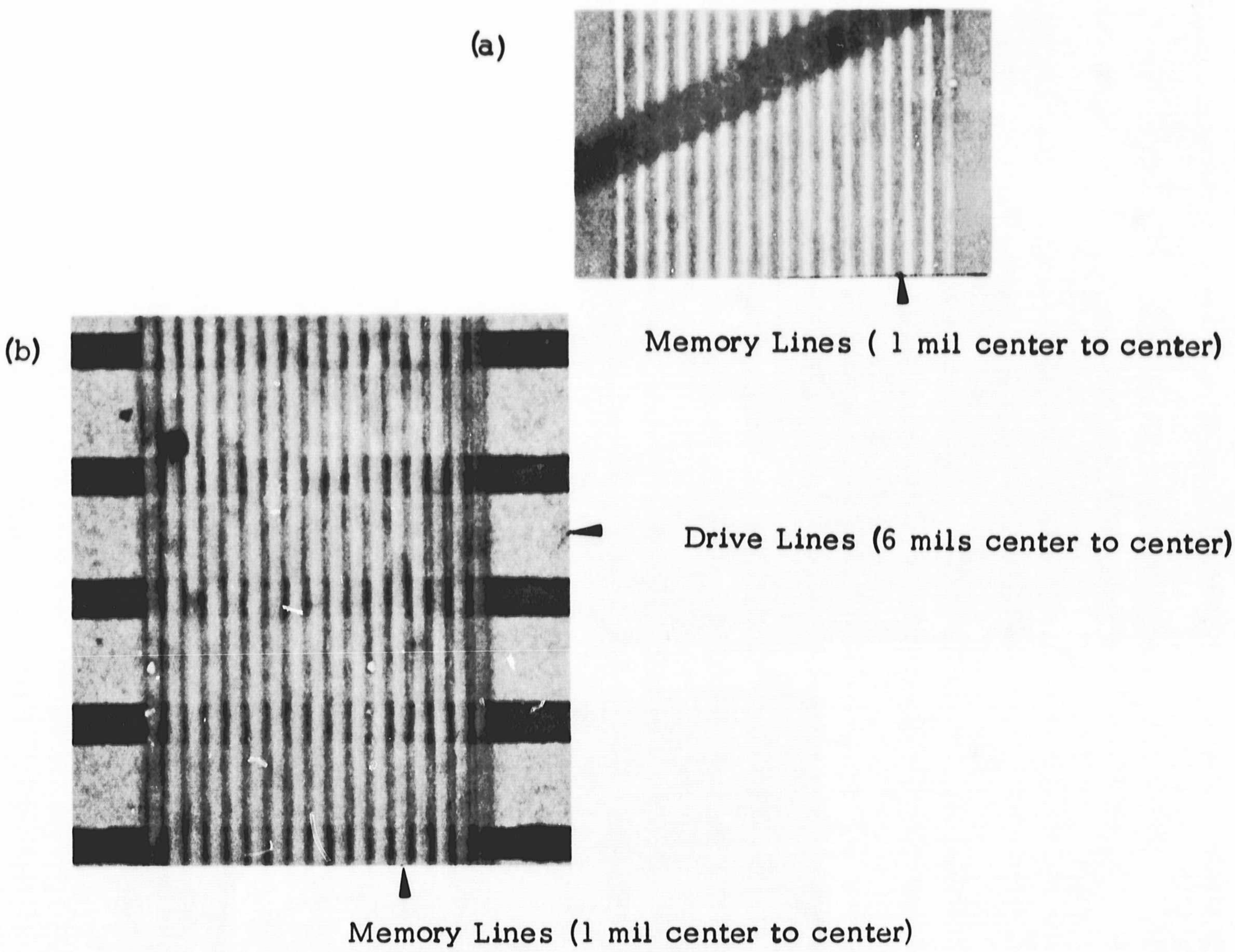

Fig. 24. Half Mil Memory Lines (Reflected Light)
(a) With Human Hair
(b) With Drive Lines

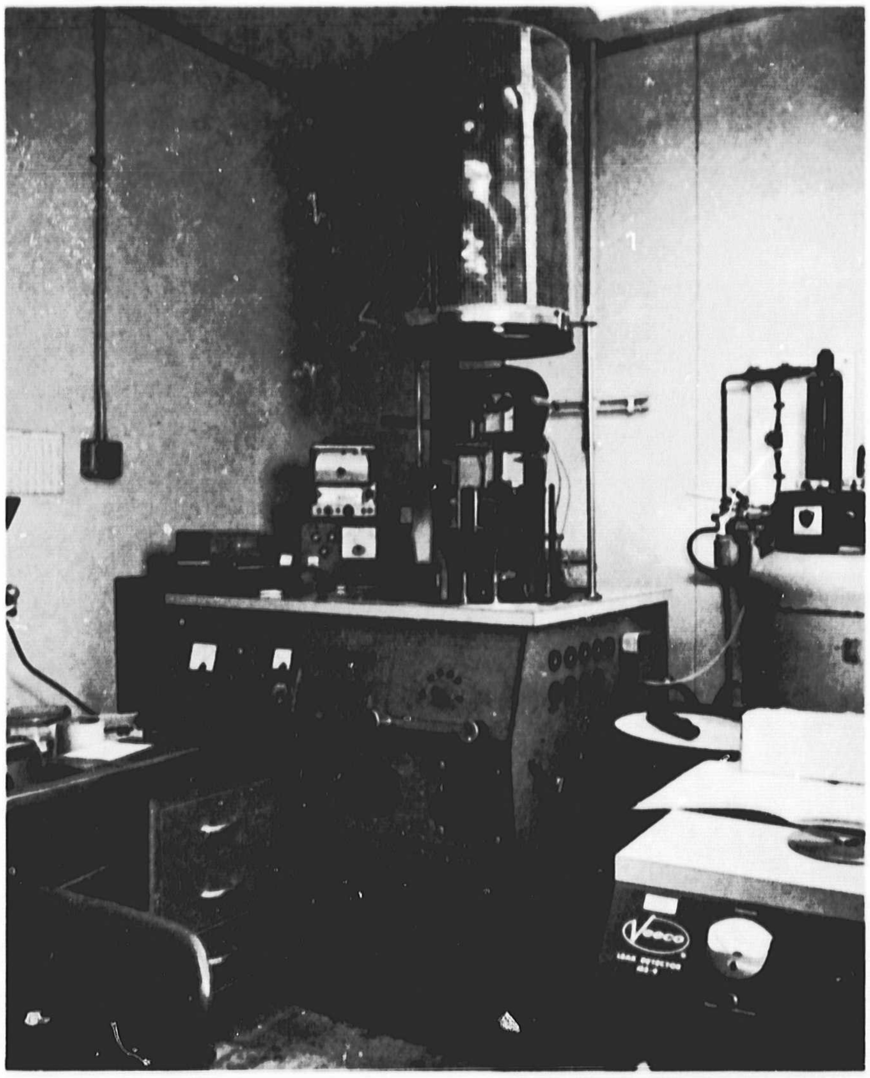

(a)

(b)

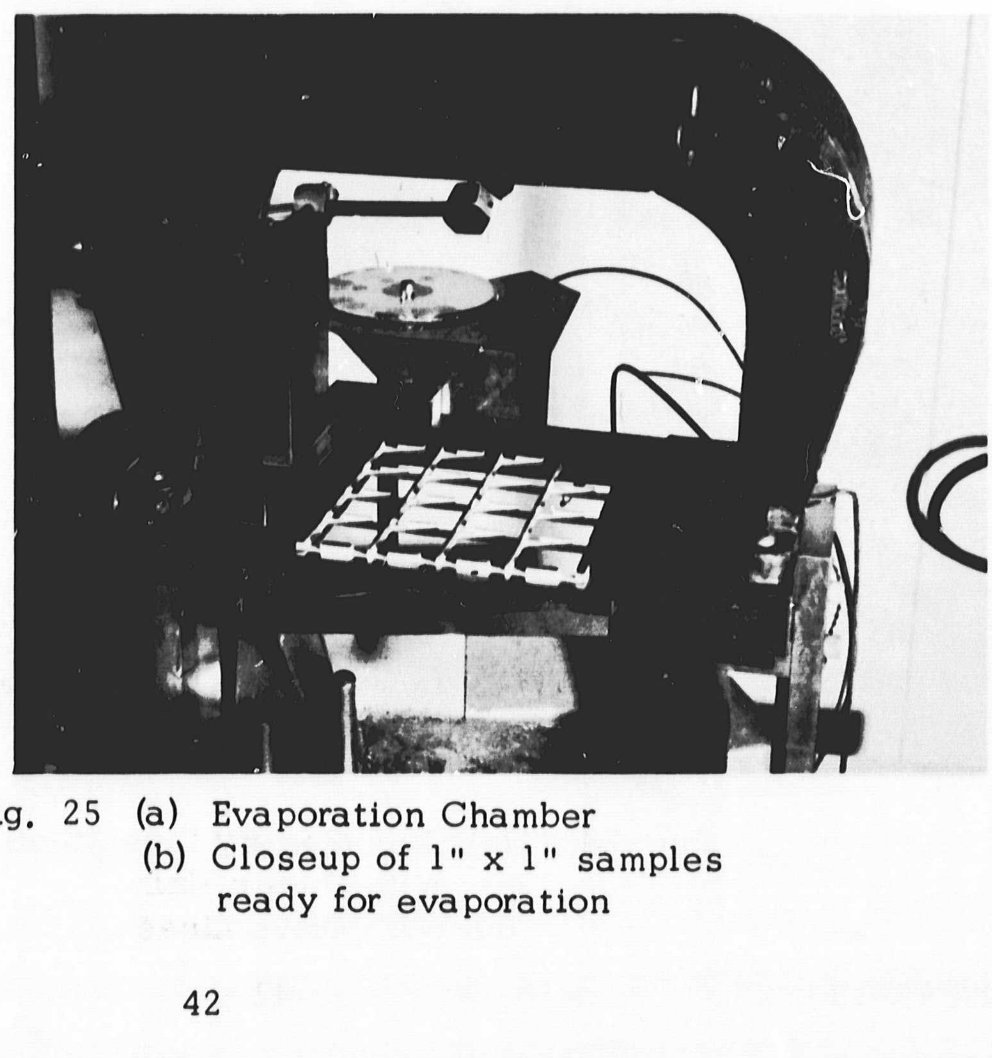

Fig. 25 (a) Evaporation Chamber
(b) Closeup of 1" x 1" samples ready for evaporation

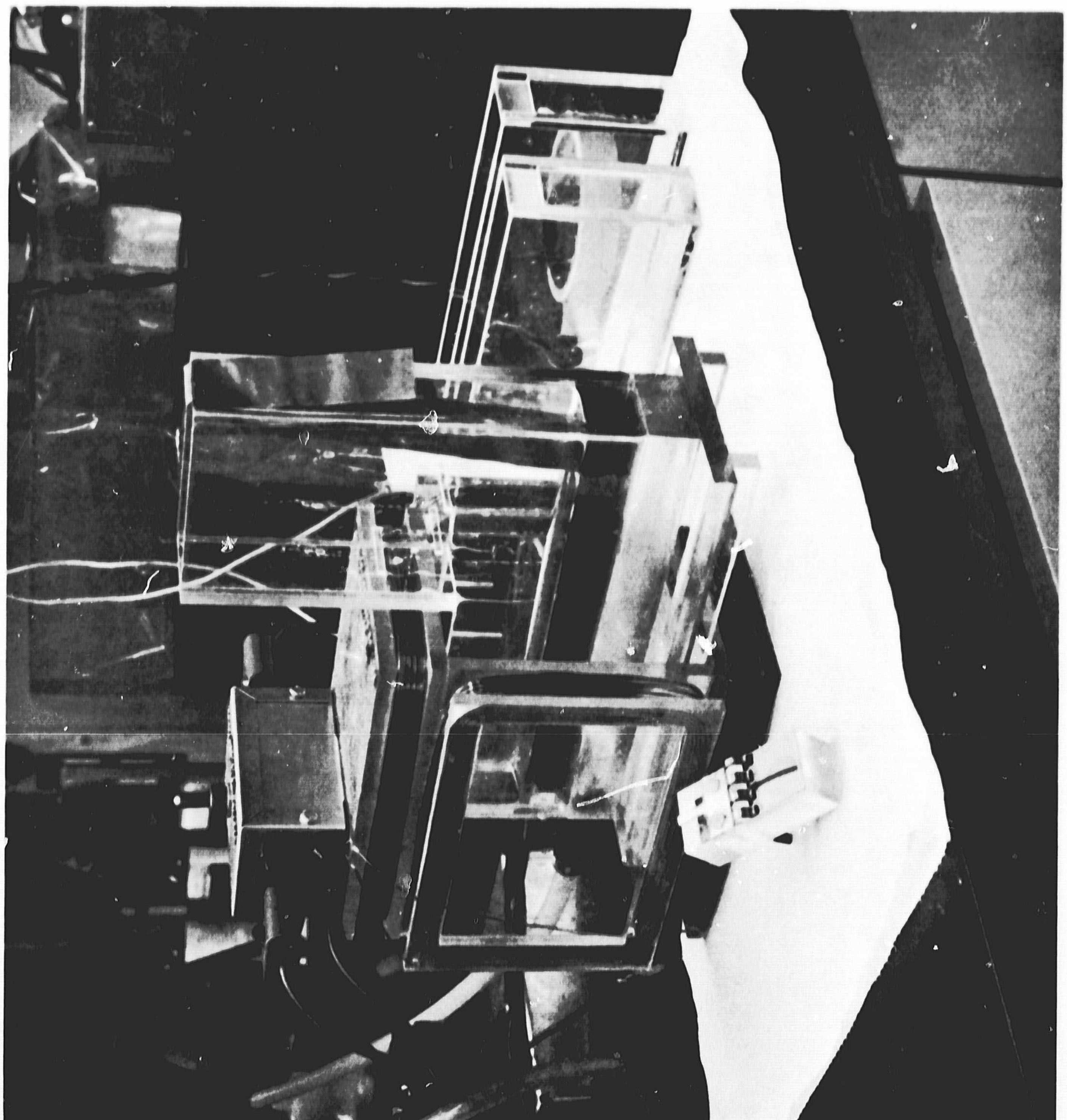

Fig. 26 Plating Tank and Helmholz Coils

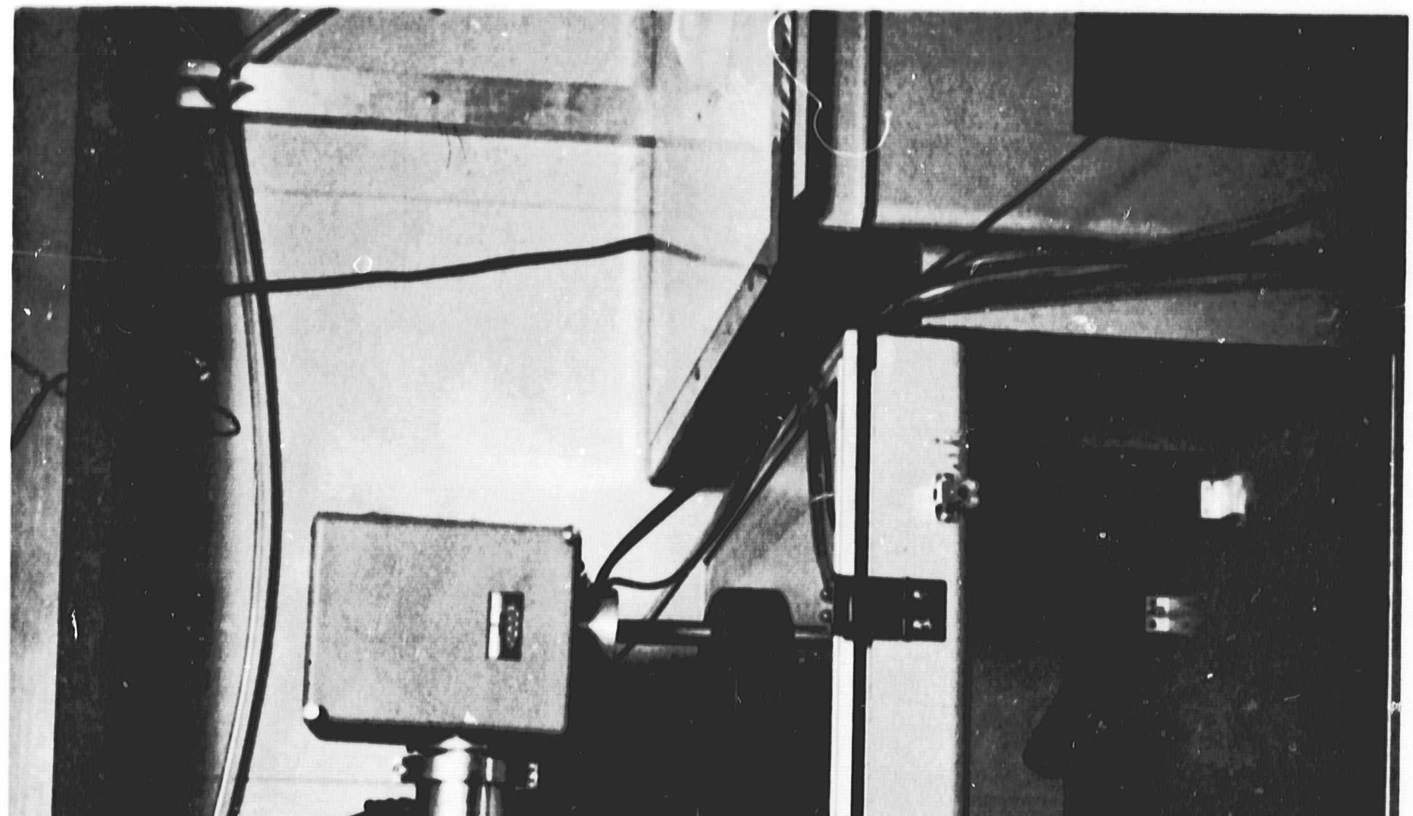

Fig. 27 Vacuum Frame and Exposure Light for Photo Masking

10.0 SUMMARY AND OUTLOOK

It was the scope of the present work to prove the feasibility of producing high density memory planes based on a closed flux structure developed by Ampex.

Since the digit line density is only fabrication-limited, it was important to show that very fine memory lines can be produced. Digit lines of .5 mil and .25 mil width have been successfully etched; a memory line density of 1000 lines per inch or even more will, therefore, be feasible.

The word line density is limited by demagnetization and creep effects. It has been demonstrated that the following bit densities are possible:

1000 Å film: 166,000 bits/inch^2
500 Å film: 250,000 bits/inch^2

In a two-spots-per-bit configuration these density figures have to be divided by two.

Electronic test results were obtained by working with wider digit lines. The memory arrays for electronic evaluation were scaled in a way to give conclusive results for the high density planes.

The following points need further investigation and are proposed for an extension of this program.

Part I (1) electronic evaluation of high density planes in DRO and NDRO mode.

(2) signal detection and noise cancellation

Part II Integration of magnetics and electronics using medium or large scale integrated circuits.

Connection of integrated circuit chips and memory array with photo-masking techniques.

APPENDIX I

MAGNETIZATION DISTRIBUTION UNDER NONUNIFORM HARD-AXIS DRIVE

1.0 Continuous Film

This case has been treated by V. V. Kobelev [2]. We derive the integral equation associated with the demagnetization problem. This yields an exact solution as long as the magnetization in the hard axis direction is below saturation. A similar integral equation will be obtained in the double film case and in the case of film elements of finite width.

Due to symmetry within the infinite plane (see Fig. 28) and because of the geometrical anisotropy of the thin film, we have to solve only a one-dimensional problem. The magnetic pole density is known to be $\rho_m = - \nabla \cdot \bar{M}$, $\bar{M}$ = magnetization vector. Since $\bar{M}$ has no component perpendicular to the film and since the magnetization varies only along the x-axis (Fig. 28)

$$\rho_m = - \frac{dM_x}{dx}$$

which is constant across the film thickness. The charge per unit length of a line charge at point x_1 becomes

$$q_\ell = - T \frac{dM_x}{dx} dx_1 \quad (1)$$

The magnetic field of a line charge at a distance $(x - x_1)$ is (in emu units);

$$dH(x) = \frac{2q_e}{x-x_1} = -2T \; \frac{dH_x}{dx} \, \frac{1}{x-x_1} \, dx_1 \qquad (2)$$

Integration of (2) yields the total demagnetizing field of a point x:

$$H(x) = -2T \int_{-\infty}^{+\infty} \frac{dM_x}{dx} \, \frac{1}{x-x_1} \, dx_1 \qquad (3)$$

The total field acting on a spin is the sum of the applied field H_a and the demagnetizing field H

$$H_T = H_a + H \qquad (4)$$

Below saturation the transverse magnetization depends linearly on the total field. It follows from the Steiner-Wohlfarth [3] model that

$$\frac{M_x}{M_s} = \frac{H_T}{H_k} \, , \qquad (5)$$

M_s = saturation magnetization

H_k = anisotropy field

Substituting (3) into (4) and using (5) we find:

$$m(x) = h_a(x) - \lambda \int_{-\infty}^{+\infty} \frac{dm_x}{dx} \, k(x-x_1) \, dx_1 \qquad (6)$$

with

$$m = \frac{M_x}{M_s} \; ; \quad h_a = \frac{H_a}{H_k} \; ; \quad \lambda = \frac{2TM_s}{H_k} \; ; \quad k = \frac{1}{x-x_1}$$

The integro-differential equation (6) is easily solved using the Fourier integral transform. * Applying the convolution theorem and the differentiation rule we find: [4]

$$m(w) = h_a(w) - jw\lambda k(w) \cdot m(w)$$

and hence for m(w)

$$m(w) = \frac{h_a(w)}{1 + jw\lambda k(w)} \tag{7}$$

The Fourier integral for the odd function 1/x is

$$-2j \int_0^\infty \frac{\sin(wx)}{x} dx = -j\pi \frac{|w|}{w}$$

hence

$$m(w) = \frac{h_a(w)}{1 + \pi |w| \lambda} \tag{8}$$

If the film is driven by a strip line in close proximity to the plane; then the applied field $h_a(x)$ can be approximated by a step function (see Fig. 29). The Fourier transform of $h_a(x)$ is

$$h_a(w) = 2 \cdot \frac{\sin(x_0 w)}{w} \tag{9}$$

---

* Kobelev solved this equation using double-sided Laplace transform.

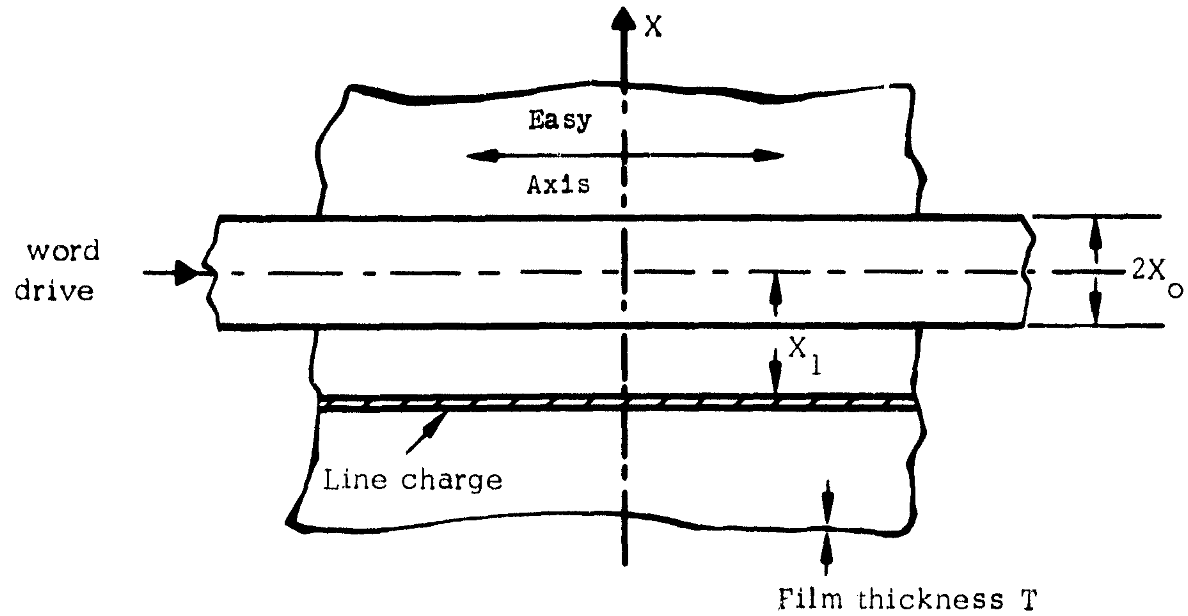

Fig. 28 Line Charge Model Continuous Film

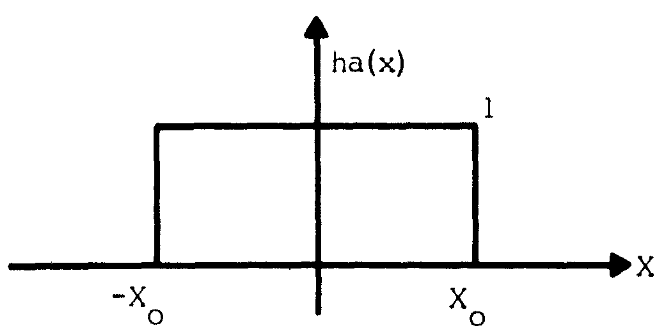

Fig. 29 Drive Field for Strip Line in Close Proximity to Film

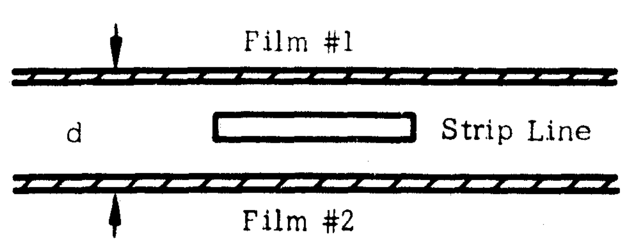

Fig. 30 Double Film Configuration

Taking the inverse transform of (8) we obtain the magnetization distribution:

$$m(x) = \frac{2}{\pi} \int_0^{\infty} \frac{\sin(x_0 w) \cos(wx)}{w(1+\lambda \pi w)} dw \tag{10}$$

2.0 Double Film Configuration

We add a second continuous film with the same characteristics ($\lambda_1 = \lambda_2$) and lay it on top of the strip line in Fig. 30. This way a structure is obtained that consists of a strip line sandwiched in between two continuous films. On both films a demagnetizing field is generated during hard drive; but together with the drive fields the demagnetizing fields of the two films have opposite signs and, therefore, lower the total demagnetizing field.

With reference to Fig. 30, we easily find the demagnetizing field component $H_{1,2}$ in Film #1, due to change in magnetization in Film #2 (and vice versa).

$$\begin{aligned} H_{1,2}(x) &= -\lambda \int_{-\infty}^{+\infty} \frac{dm^{(2)}}{dx} \frac{x-x_1}{(x-x_1)^2+d^2} dx_1 \\ H_{2,1}(x) &= -\lambda \int_{-\infty}^{+\infty} \frac{dm^{(1)}}{dx} \frac{x-x_1}{(x-x_1)^2+d^2} dx_1 \end{aligned} \tag{11}$$

The self-demagnetizing fields H_{11} and H_{22} are readily obtained from (3). In the double film configuration the magnetization distribution is found by solving two coupled integral equations:

$$m^{(1)}(x) = h_{a_1}(x) - \lambda \int_{-\infty}^{+\infty} \frac{dm^{(1)}}{dx} k_1(x-x_1)dx_1 - \lambda \int_{-\infty}^{+\infty} \frac{dm^{(2)}}{dx} k_2(x-x_1)dx_1 \tag{12}$$

$$m^{(2)}(x) = h_{a_2}(x) - \lambda \int_{-\infty}^{+\infty} \frac{dm^{(2)}}{dx} k_1(x-x_1)dx_1 - \lambda \int_{-\infty}^{+\infty} \frac{dm^{(1)}}{dx} k_2(x-x_1)dx_1 \tag{13}$$

with

$$k_1 = 1/x \quad ; \quad k_2 = x/(x^2+d^2) \tag{14}$$

Taking the Fourier transform of both the equations (12) and (13) yields a pair of linear equations with the solution for symmetric drive ($ha_1 = h$; $ha_2 = -h$):

$$m^{(1)} = \frac{h(w)}{1 + jw\lambda \Delta k(w)} \quad ; \quad \Delta k = k_1 - k_2 \tag{15}$$

$$m^{(2)} = -m^{(1)}$$

The Fourier transform of $\quad \Delta k = 1/x - x/(x^2+d^2)$

is found to be $\quad \Delta k(w) = -j\frac{|w|}{w}\pi\left(1 - e^{-|w|d}\right)$

Assuming h(x) to be an even function and taking the inverse Fourier transform of (15)

$$m^{(1)}(x) = \frac{1}{\pi}\int_0^\infty \frac{h(w)\cos(wx)}{1+\pi\lambda w(1-e^{-wd})}\,dw \qquad (16)$$
$$m^{(2)}(x) = -m^{(1)}(x)$$

Once we know h(w), which for small d is suitably approximated by (9), then the magnetization distribution during hard drive is given for both films by equations (16). For d = ∞ and keeping the same drive field, we go back to the solution for a single film; the limiting case d = 0 gives $m^{(1)}(x) = -m^{(2)}(x) = h(x)$, which means complete absence of any demagnetizing fields (perfectly closed magnetic path).

3.0 Coupled Film Element of Finite Width

Instead of a continuous film we now consider film elements consisting of closed flux structures of finite width 2ℓ. (See Fig. 31a.) To compute the magnetization distribution on the x-axis (see Fig. 31b) we again apply the line charge model having now finite line charges of length 2ℓ. The linear charge density along the line charge is assumed to be constant, which is an approximation:

$$dq_\ell = -T\frac{dM_x}{dx}\,dx_1\,d\xi \qquad (17)$$

Using the model of Fig. 31b we find for field contribution of one line charge at a distance $(x - x_1)$

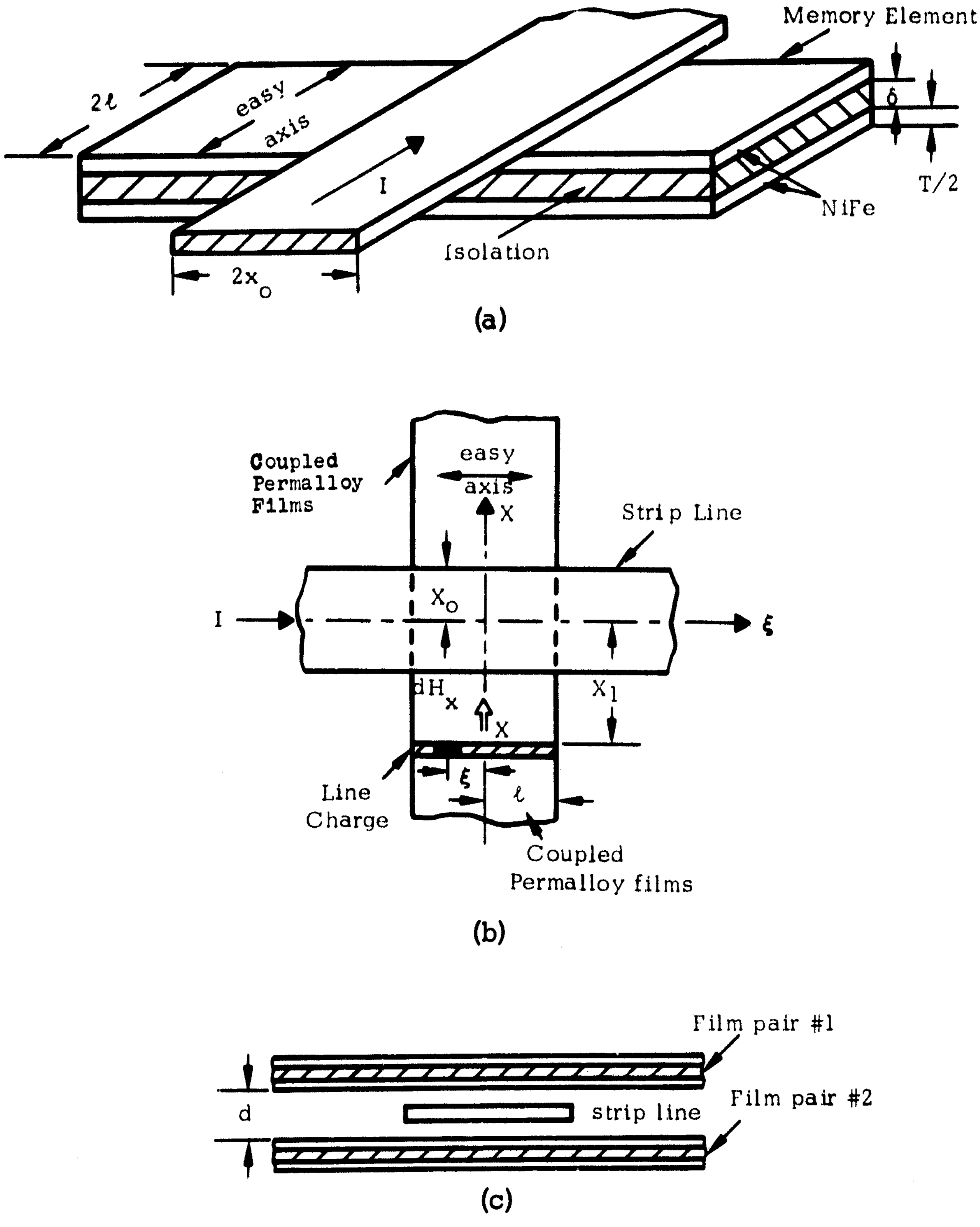

Fig. 31 Film and Drive Line Geometry

(a) Memory element and hard axis drive line
(b) Model for computation
(c) Two element configuration for demagnetization compensation

$$dH(x) = \int_{-l}^{+l} \frac{dq_\xi}{(x-x_1)^2+\xi^2} \, \frac{x-x_1}{\sqrt{(x-x_1)^2+\xi^2}}$$

and substituting (17)

$$dH(x) = -\frac{dM_x}{dx} T \, dx_1 \int_{-l}^{l} \frac{x-x_1}{\left[(x-x_1)^2+\xi^2\right]^{3/2}} \, d\xi \tag{18}$$

$$= -2T \frac{dM_x}{dx} \frac{dx_1}{(x-x_1)\sqrt{1+\left(\frac{x-x_1}{l}\right)^2}}$$

Equation (18) replaces (2). The field contribution of a line charge at a distance r is no longer proportional to 1/r but to $1/r\sqrt{1 + (r/e)^2}$. As under III, we investigate a double element configuration (see Fig. 31c). Equation (15) gives also the solution to this problem in the transformation domain if we change the kernels k_1 and k_2 accordingly:

$$k_{1,l} = \frac{1}{x\sqrt{1+(x/l)^2}} \; ; \; k_{2,l} = \frac{x}{x^2+d^2} \, \frac{1}{\sqrt{1+\frac{x^2+d^2}{l^2}}} \tag{19}$$

$$\Delta k = k_{1,l} - k_{2,l} = \frac{1}{x\sqrt{1+(x/l)^2}} \left[1 - \frac{x^2}{x^2+d^2} \sqrt{\frac{x^2+l^2}{x^2+d^2+l^2}}\right]$$

The magnetization distribution is the inverse transform of (15):

$$m^{(1)}(x) = \frac{1}{\pi} \int_0^{\infty} \frac{k(w) \cos(wx)}{1 + j\lambda w \Delta k(w)} dw \tag{20}$$

In this case, however, it is less trivial to find the transform $\Delta k(w)$. For the general case, the transform has to be carried out numerically. (Results see Fig. 10.)

APPENDIX II
THEORY OF THE RF SENSING

A domain is exposed to an rf hard-axis drive field

$H(t) = H_o \cdot \sin wt$

The total flux of the domain is

$\phi_o = W \cdot T \cdot M_s$, W = domain width
T = film thickness
M_s = saturation moment

During hard-axis drive the magnetic moment is being rotated by an angle φ with respect to the easy axis. The total flux as a function of time is, therefore,

$\phi(t) = \phi_o \cdot \cos\varphi = \phi_o \cdot \sqrt{1-\sin^2\varphi}$; below saturation

$\sin\varphi = \frac{H(t)}{H_k}$; H_k = anistropy field

$$\phi(t) = \phi_o \sqrt{1 - (H/H_k)^2} \approx \phi_o \left[1 - 1/2\left(\frac{H(t)}{H_k}\right)^2\right]$$

since $H < H_k$.

The induced voltage becomes:

$$V_i = \frac{d\phi}{dt} \approx -\pi \phi_o \nu \left(\frac{H_o}{H_k}\right)^2 \cdot \sin 2 \cdot wt; \; w = 2\pi\nu$$

ν: frequency of the drive current.

The frequency of the sense signal is twice the frequency of the hard-axis drive; hence, by using narrowband amplification, very good S/N ratios are obtainable. Switching the domain to its opposite polarity gives rise to a 180° phase shift of the sense signal. Thus a "1-signal" and a "0-signal" show a phase difference of 180°.

APPENDIX III

DRIVE AND SENSE ELECTRONICS FOR THE ELECTRONIC TESTING

1.0 RF Readout (Fig. 32 thru 33.)

To test the sample in the RF readout mode, we drive the word line with a 20 Mcs sine wave. The induced readout signals on the digit lines should have twice the frequency of the drive. To separate the 2nd harmonic from its fundamental which is coupled into the digit lines, the sense outputs are filtered through two bandpass Tchebysheff filters which are designed with the following characteristics:

center frequency = 40 Mcs
bandwidth = 20 Mcs
skirt rejection = 40 db @ 20 Mcs and 60 Mcs
ripple ratio = 3 db
characteristics impedance = 50 Ω

The outputs of the filters are amplified and displayed on a dual beam scope at the same time than the fundamental, for phase reference.

By driving the two digit lines with a ±200 mA D. C. current, one can change the state of the magnetization of the films, and therefore change the relative phase between the two R. F. readouts.

2.0 Wideband Readout (Fig. 34)

The digit current drivers comprise two separate pairs of drivers. The T_1 and T_2 pair provides the normal write current and/or a specified number of read disturb currents in both directions; and the other T_3, T_4 pair furnishes a large (+) or (-) prewrite disturb current.

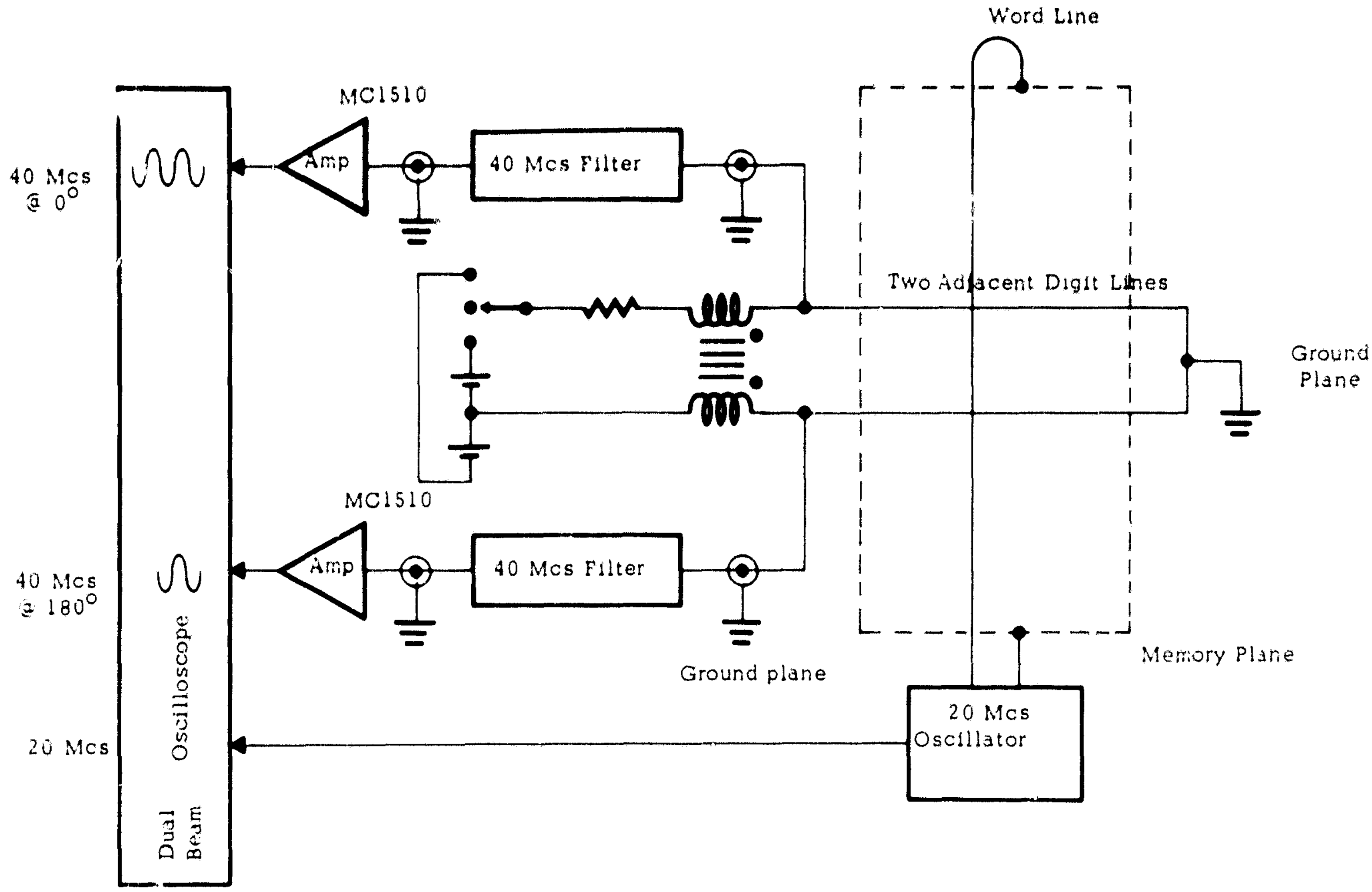

Fig. 32 R. F. Readout

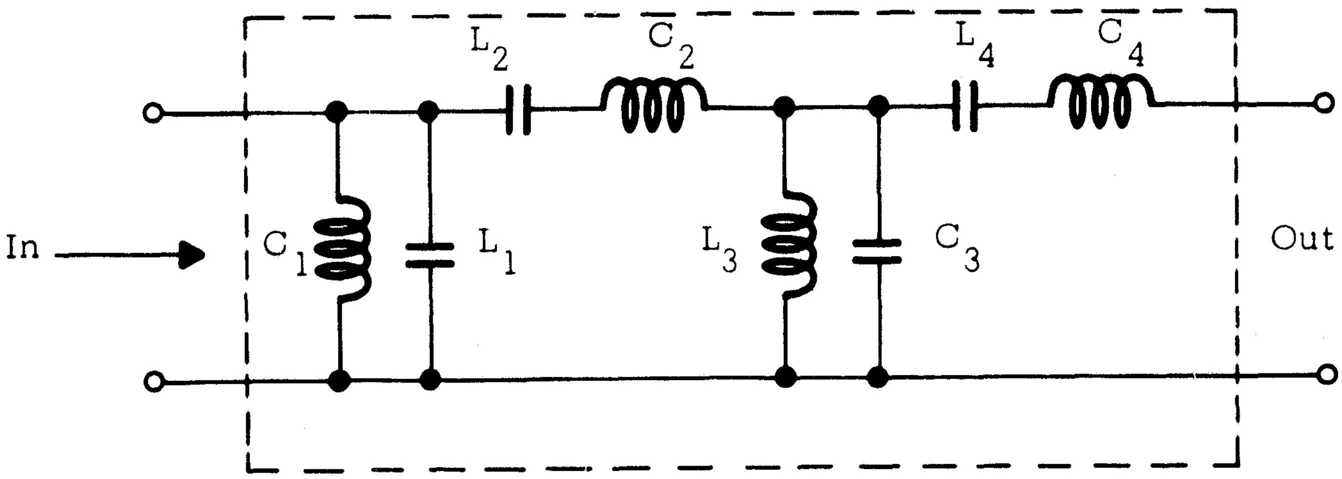

C_1

$C_1 = 99$ pf $C_2 = 19$ pf $C_3 = 119$ pf $C_4 = 24$ pf
$L_1 = 0.193\ \mu H$ $L_2 = 1.72\ \mu H$ $L_3 = 0.133\ \mu H$ L_4 . $0.133\ \mu H$

Fig. 33 Filter

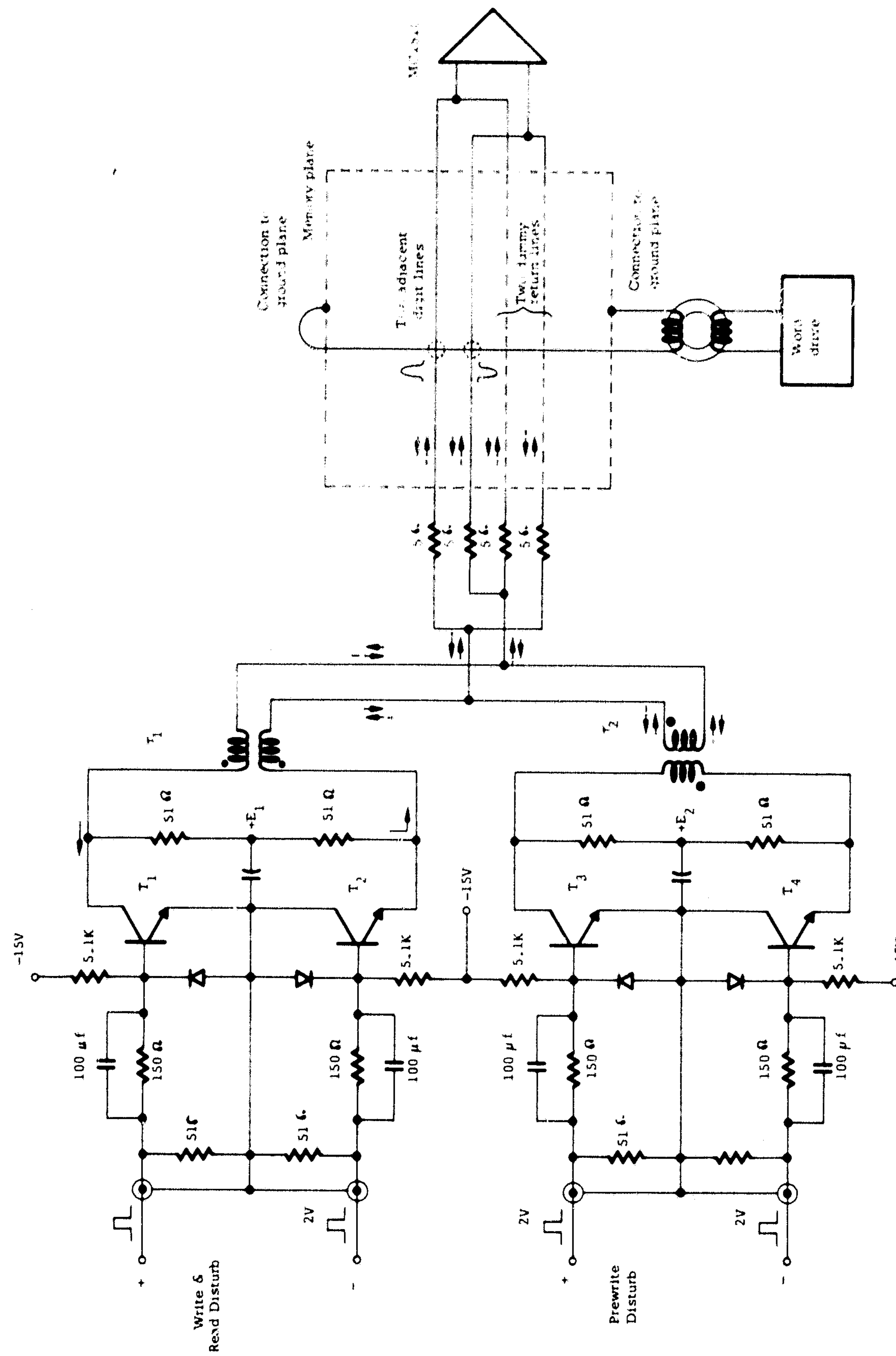

T_1 and T_2 are 014-506
T_3 and T_4 are 014-547

NOTICE: Ground plane is kept floating with respect to the system ground

Fig. 34 Digit Current Drivers

If T_1 is turned on, a current will flow from the variable supply E_1 along the path indicated by the black arrows into the two branches of the bridge, and return to ground through T_1. The current is reversed if T_2 is turned on. By activating T_1 and T_2 in a proper sequence one can generate the desired write and read disturb digit current pattern. Their amplitudes can be changed simultaneously by varying E_1. Similarly, one can inject the large prewrite disturb current into the bridge by turning on either T_3 or T_4. The two transformers τ_1 and τ_2 isolate the two pair of drivers from each other and also present high impedance return paths to the sense signals. The word driver is coupled to the word line (with ground plane as return path), through a pulse transformer. System ground and word line ground are then kept separated, for minimum readout noise.

Proper overlapping between with digit current and word current pulses allows writing on the two spots at the intersection of the two adjacent bit lines and the corresponding word line.

During readout, word current alone is turned on. The switching of the two spots induces two opposite sense pulses travelling along the digit lines to the input of a differential amplifier whose output is displayed on the scope.

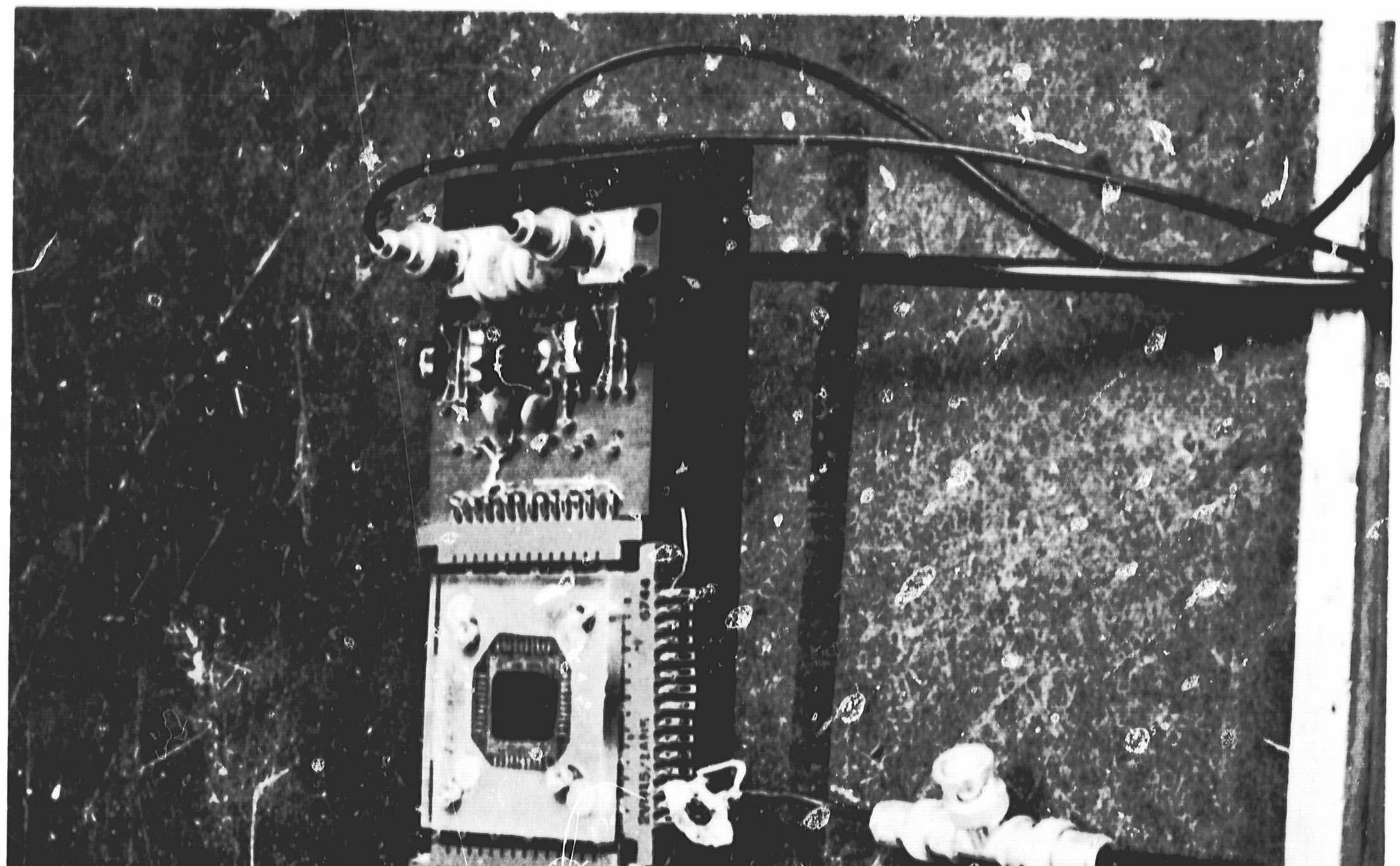

Fig. 35 Jig and Circuits for Electronic Evaluation

PRECEDING PAGE BLANK NOT FILMED.

REFERENCES

[1] Coren, R.L., "Shape Demagnetizing Effects in Permalloy Films," Journal of Applied Physics, Vol. 37, No. 1, Jan. 1966.

[2] Kobelev, V.V., "Ferromagnetic Films in Nonuniform Fields," Phys. Stat. Sol. 17, 381, 1966.

[3] Middelhoek, S., "Ferromagnetic Domains in Thin Ni-Fe Films," Drukkerij Wed. Co. Van Soest N.V., Amsterdam, 1961.

[4] Titschmarsh, E.C., "Introduction to the Theory of Fourier Integrals," Claredon Press, Oxford, 1948.